



國立臺灣大學醫學院免疫學研究所

博士論文

Graduate Institute of Immunology

College of Medicine

National Taiwan University

Doctoral Dissertation

以生物資訊學模式探討腫瘤微環境對頭頸癌病患接受

免疫調節點抑制劑複方治療之效應研究

Bioinformatic approach to tumor microenvironment in
head and neck squamous cell carcinoma patients taking
immune checkpoint inhibitor combination therapy

高祥豐

Hsiang-Fong Kao

指導教授： 賈景山博士

洪瑞隆博士

Advisor: Jean-San Chia, Ph.D.

Ruey-Long Hong, Ph.D.

中華民國111年4月

April, 2022

國立臺灣大學博士學位論文
口試委員會審定書

PHD DISSERTATION ACCEPTANCE CERTIFICATE
NATIONAL TAIWAN UNIVERSITY

以生物資訊學模式探討腫瘤微環境對頭頸癌病患接受免疫調節點抑制劑複方治療之效應研究

Bioinformatic approach to tumor microenvironment in head and neck squamous cell carcinoma patients taking immune checkpoint inhibitor combination therapy

本論文係高祥豐（學號 D04449005）在國立臺灣大學醫學院免疫學研究所完成之博士學位論文，於民國 111 年 4 月 9 日承下列考試委員審查通過及口試及格，特此證明。

The undersigned, appointed by the Institute of Immunology, College of Medicine, National Taiwan University, on 9th April 2022, have examined a PhD dissertation entitled above presented by Hsiang-Fong Kao (student ID: D04449005) candidate and hereby certify that it is worthy of acceptance.

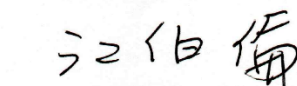
口試委員 Oral examination committee:

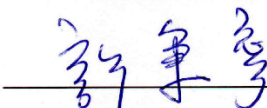


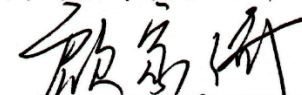
(指導教授 Advisor)

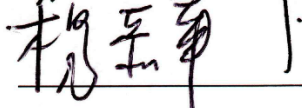


(共同指導教授 Co-Advisor)



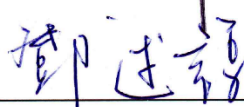








系主任/所長 Director:



Acknowledgement



感謝所有參與臨床試驗以及臨床觀察性研究的病人及家屬。

感謝賈景山教授與洪瑞隆教授這些年來的指導，支持與鼓勵。

賈景山教授 實驗室

高孔奇，連惠婷，魏鈴穎醫師

洪瑞隆教授 研究團隊

廖斌志醫師，黃懷正醫師，洪苑菁，詹靜宜

台大醫院，台大醫院附設癌醫中心醫院

腫瘤內科部 許駿教授

病理科 黃彥霖醫師

耳鼻喉科 陳俊男醫師，陳贈成醫師

亞東醫院 內科部 醫學研究部

邱彥霖醫師

在爭取臨床試驗，以及研究的道路上，一路支持鼓勵的夥伴與朋友

Yu-Ming Chang, Yu-Chieh (Peter) Wang, Kevin Chueh, Dennis Chin-Lun Huang, Yan-Ping Liu, Kuei-Fang Wang, Chie-Yu Charles Liao, Kuan-I Lee, Chengju Lulu Wang, Shoung-Hui Tsai, Shang-Yun Liu, and Yu-Ting Huang

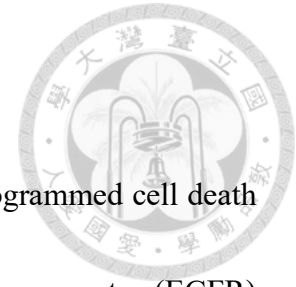
中文摘要



腫瘤微環境(tumor microenvironment)的調控被認為可增加計畫性死亡蛋白-受體 1 抗體 (anti-programmed cell death protein 1 antibody, or anti PD-1 antibody) 的治療效果。在細胞與動物試驗中發現，抑制表皮生長因子受體(epithelial growth factor receptor, EGFR)可誘發腫瘤呈現抗原，並增強 anti-PD-1 的效果。本研究計畫假設，藉由合併使用 EGFR 酪胺酸激酶抑制劑(tyrosine kinase inhibitor) afatinib 以及 pembrolizumab 免疫調節點抑制劑，可增進免疫治療於頭頸癌的成效。本研究的臨床試驗(NCT03695510)，完成 29 位病患的收案與治療。整體腫瘤達客觀縮小的比例為 41.4%。於檢體研究中發現，在治療後，腫瘤微環境內之抗原表現及免疫活化之相關基因組的表現有顯著上升。在腫瘤基因突變分析中，我們發現未改變的 methylthioadenosine phosphorylase (unaltered MTAP) 者的檢體有較偏向炎性反應的腫瘤微環境，有較佳的治療反應及治療預後。我們利用 cytometry by time-of-flight (CyTOF) 分析 chemokine receptor，可以觀察到不同的異質性存在於各類型細胞中。本研究藉由臨床試驗，證實 afatinib-pembrolizumab 對於頭頸癌病患的治療成效。腫瘤微環境的研究證實此治療可增加微環境內的抗原表現。同時找到 MTAP 為可能的預後因子。接下來我們將繼續發展其他可能的人體免疫學多面向生物資訊學分析模式，建立頭頸癌免疫癌症治療轉譯醫學研究模式。

關鍵字: 頭頸癌，癌症免疫治療，腫瘤微環境，生物資訊學，afatinib，pembrolizumab

Abstract



Tumor microenvironment (TME) modulation may improve programmed cell death 1 (PD-1)-targeted antibody therapy efficacy. Epidermal growth factor receptor (EGFR) pathway inhibition upregulates tumor antigen presentation machinery within the TME in preclinical models. We hypothesized that the irreversible EGFR tyrosine kinase inhibitor afatinib combined with pembrolizumab (anti-PD-1) would improve outcomes in head and neck squamous cell carcinoma (HNSCC) patients. A Phase II trial (NCT03695510) including 29 eligible patients met its primary endpoint by improving the objective partial response (objective response rate, 41.4%). The post-treatment, paired-tissue analysis revealed afatinib plus pembrolizumab upregulated antigen presentation machinery and increased inflammation in TME. Tumors with unaltered methyl-thioadenosine phosphorylase (MTAP) had an inflamed TME and predicted better clinical benefits. Proteomics analysis of PD-1⁺ T cells using cytometry by time-of-flight (CyTOF) identified the chemokine receptor landscape. In conclusion, afatinib augments pembrolizumab therapy and improves the ORR in HNSCC patients by upregulating antigen presentation machinery in TME. Unaltered MTAP may predict a favorable TME and serve as a predictive biomarker for anti-PD-1 therapy.

Keywords: head and neck squamous cell carcinoma, cancer immunotherapy, tumor microenvironment, bioinformatics, afatinib, pembrolizumab

Contents



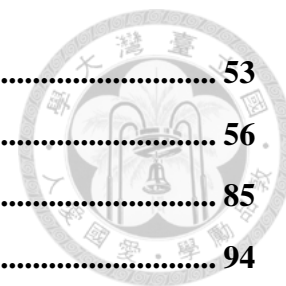
口試委員會審訂書	i
Acknowledgement.....	ii
中文摘要	iii
Abstract	iv
Contents	v
List of Tables.....	ix
List of Figures	ix
Chapter 1 Introduction.....	1
1.1 Head and neck squamous cell carcinoma in Taiwan	1
1.2 Treatment for recurrent or metastatic HNSCC in the pre- immunotherapy era	2
1.3 Immune checkpoint inhibitors for HNSCC	3
1.4 Tumor microenvironment and genomics.....	4
1.4.1 Immune cells in the tumor microenvironment.....	4
1.4.2 Cancer genomics and the tumor microenvironment.....	6
1.4.3 Lessons from research in the tumor microenvironment: Finding biomarkers	7
1.4.4 Bioinformatics and multi-omics approaches to human immunology.....	8
1.5 Anti-PD-1 combination therapy in HNSCC: Rationale and current landscape.....	10
1.5.1 Overcoming intrinsic resistance in anti-PD-1 therapy	10
1.5.2 The role of the antigen presentation machinery in anti-PD-1 therapies.....	11
1.5.3 Anti-PD-1 therapy combined with chemotherapy: Current landscapes and unmet needs	11
1.6 The role of the EGFR signaling pathway in HNSCC immunotherapy	12
Chapter 2 Hypothesis and specific aims	14
2.1 Hypothesis	14
2.2 Specific aims.....	14
Chapter 3 Materials and methods	15



3.1	Clinical trials.....	15
3.1.1	Study approval.....	15
3.1.2	Study design.....	15
3.1.3	Efficacy assessment.....	16
3.1.4	mRNA expression analysis.....	17
3.1.5	Comprehensive genomic profiling	18
3.1.6	TCGA HNSCC data acquisition and analysis	19
3.1.7	PD-L1 testing.....	19
3.1.8	Statistical analysis.....	20
3.2	Deciphering the tumor microenvironment in HNSCC	21
3.2.1	Patient population and specimen collection	21
3.2.2	Isolation of peripheral blood mononuclear cells and T cells.....	22
3.2.3	Isolation of tumor-infiltrating lymphocytes.....	23
3.2.4	FACS staining and analysis.....	23
3.2.5	Flow cytometry using mass cytometry	24
Chapter 4	Results.....	26
4.1	Clinical studies.....	26
4.1.1	Afatinib plus pembrolizumab therapy showed improved efficacy in HNSCC patients.....	26
4.1.2	The toxicities associated with afatinib plus pembrolizumab therapy were tolerable	27
4.1.3	Biomarker analysis	27
4.1.3.1	mRNA expression analysis in paired biopsy tissues showed that afatinib plus pembrolizumab treatment augments antigen presentation machinery	27
4.1.3.2	Targeted gene sequencing analysis revealed that unaltered methylthioadenosine phosphorylase could serve as a potential biomarker for response to therapy	29
4.1.3.3	GSEA analysis using study data and TCGA data showed that tumors with unaltered MTAP presented an inflamed microenvironment	30
4.1.3.4	Post-progression, targeted gene sequence analysis revealed acquired loss	

	of MTAP in a patient with disease progression after initial response.....	31
4.1.3.5	A high response rate is observed in patients with high PD-L1 expression.	32
4.2	Microenvironment study using a multiplexed proteomics approach.....	32
4.2.1	Pilot experiment using CyTOF and trouble-shooting.....	32
4.2.2	CyTOF study using cancer patient tissues.....	36
4.2.2.1	Differences in CD3 ⁺ T cells between PBMCs and TILs.....	36
Chapter 5	Discussion	38
-	Afatinib plus pembrolizumab therapy is an effective option for patients with HNSCC	38
-	Multi-omics analysis of paired tissue samples revealed the upregulation of antigen presentation machinery and the stimulation of immune functions in the tumor microenvironment.....	38
-	Genetics studies and post-progression biopsies revealed that unaltered MTAP may regulate immune functions in the tumor microenvironment	40
-	The outlook for anti-PD-1 combination therapy in HNSCC	41
-	Next steps: extend the DoR achieved for afatinib plus pembrolizumab combination therapy	42
-	Mechanisms of acquired resistance to afatinib plus pembrolizumab combination therapy: what do we know?	43
-	Toxicities associated with afatinib plus pembrolizumab therapy in HNSCC.....	45
-	Limitations of this prospective study.....	46
-	A journey in CyTOF study: lessons learned	48
-	Conclusion	49
Chapter 6	Future works	50
6.1	Real-world analysis of anti-PD-1 therapy in patients with HNSCC and accompanying biomarker analysis.....	50
6.2	Ribociclib, an anti-CDK4/6 inhibitor, combined with anti-PD-1 for HNSCC treatment	50
6.3	Personalized anti-PD-1 combination therapy in patients with HNSCC	52

Chapter 7 Tables	53
Chapter 8 Figures	56
Chapter 9 Reference	85
Chapter 10 Appendix	94
10.1 Journal papers related with this dissertation.....	94
10.2 Open data of the study	94



List of Tables

Table 1	Patient characteristics	53
Table 2	Treatment related adverse events	55



List of Figures

Figure 1	Clinical response rate to afatinib plus pembrolizumab therapy in HNSCC patients	56
Figure 2	Clinical efficacy of afatinib plus pembrolizumab therapy in HNSCC patients: progression-free survival.....	57
Figure 3	Clinical efficacy of afatinib plus pembrolizumab therapy in HNSCC patients: overall survival.....	58
Figure 4	Clinical efficacy of afatinib plus pembrolizumab treatment in HNSCC patients: the duration of response in responders.....	59
Figure 5	Differential analysis of mRNA expression between paired tissue samples	60
Figure 6	Increased mRNA expression in post-treatment specimens	61
Figure 7	Decreased mRNA expression in post-treatment specimens.....	62
Figure 8	Gene network analysis showing the central role of upregulating antigen presentation machinery in the response to afatinib plus pembrolizumab treatment.....	63



Figure 9 Changes in the T cell fractions within the tumor microenvironment after therapy 64

Figure 10 Changes in B and plasma cells in the tumor microenvironment after therapy ..
..... 65

Figure 11 The changes in myeloid cell populations in the tumor microenvironment after
therapy..... 66

Figure 12 Gene set enrichment analysis of paired tissue mRNA samples 67

Figure 13 Leading-edge analysis of three gene sets with immune cell regulatory functions.
..... 68

Figure 14 Targeted gene mutation analysis. 69

Figure 15 Survival analysis according to *MTAP* status: progression-free survival. 70

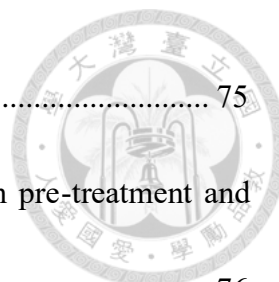
Figure 16 Survival analysis according to *MTAP* status: overall survival 71

Figure 17 Comparing patients with altered *MTAP* vs. unaltered *MTAP* by gene set
enrichment analysis..... 72

Figure 18 CIBERSORTx analysis comparing altered and unaltered *MTAP* populations ..
..... 73

Figure 19 CIBERSORTx analysis comparing the abundance of lymphocytes in patients
with altered or unaltered *MTAP*. 74

Figure 20 CIBERSORTx analysis comparing the abundance of myeloid cells in patients



with altered or unaltered <i>MTAP</i>	75
Figure 21 Differences in mutation allele frequency (MAF) between pre-treatment and post-progression specimens.	76
Figure 22 CyTOF pilot experiment	77
Figure 23 t-SNE analysis of peripheral blood mononuclear cells	78
Figure 24 SPADE analysis of peripheral blood mononuclear cells.....	79
Figure 25 Cell-ID 20-Plex Pd barcoding kit analysis.....	80
Figure 26 T helper cell location on the t-SNE map of CD4 ⁺ T cells.	81
Figure 27 Panel design for CyTOF analysis.....	82
Figure 28 Summary of results for the CyTOF study of peripheral blood mononuclear cells in HNSCC patients.....	83
Figure 29 Summary of results for the CyTOF study of tumor-infiltrating lymphocytes in HNSCC patients.....	84

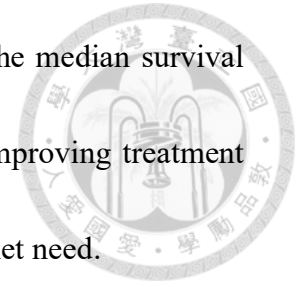
Chapter 1 Introduction



1.1 Head and neck squamous cell carcinoma in Taiwan

Head and neck squamous cell carcinoma (HNSCC) is a commonly encountered cancer in Taiwan. In 2011, approximately 6,800 new patients were diagnosed with HNSCC in Taiwan, and approximately 2,500 patients died due to this disease [1]. Some potential risk factors for head and neck cancer in Taiwan include the consumption of betel nuts, cigarettes, or alcohol. Approximately 85% of HNSCC patients in Taiwan had habits of consuming betel nuts, cigarettes, or alcohol [2]. Human papilloma virus (HPV) is another possible risk factor associated with HNSCC, especially oropharyngeal cancer [3]. Despite aggressive treatment options, the prognosis of HNSCC patients remains dismal. HNSCC treatment requires a multi-modal approach. Surgical tumor resection and lymph node dissection are the most effective treatments for patients with HNSCC. In high-risk patients, defined as those with positive resection margins, more than two metastatic lymph nodes, or extracapsular extension, concurrent chemoradiation with cisplatin is mandatory following surgery [4, 5]. However, the potential for recurrence remains high, with a 10-year locoregional failure-free survival rate of only 22.3% and an overall survival rate of only 29.1% [6]. In patients who are ineligible for surgery, definitive concurrent chemoradiation is the treatment of choice,

which is associated with a substantial risk of recurrence [7, 8]. The median survival period for inoperable oral cavity cancer is only 12 months [9]. Improving treatment options among patients with HNSCC cancer represents a great unmet need.



1.2 Treatment for recurrent or metastatic HNSCC in the pre-immunotherapy era

In patients with recurrent or metastatic HNSCC, cisplatin and fluorouracil are the first-line treatment, associated with an overall response rate of 20% and a median progression-free survival time of 3.3 months [10]. Epidermal growth factor receptor (EGFR) is highly expressed in HNSCC, and increased EGFR expression levels are associated with poor outcomes [11, 12]. Cetuximab, an EGFR-targeting monoclonal antibody, was the first immunotherapy agent developed for HNSCC treatment. Cetuximab combined with radiotherapy can prolong the median overall survival time from 29.3 months to 49.0 months ($p = 0.018$) [13]. In patients with recurrent or metastatic HNSCC, adding cetuximab to cisplatin plus fluorouracil improves the objective response rate from 20% to 36% ($p < 0.001$) and prolongs the median overall survival time from 7.4 to 10.1 months ($p = 0.04$) [10]. Despite these improvements in treatment modalities, the prognosis of patients with advanced-stage HNSCC is still poor, even after a series of intensive treatments, indicating a great unmet need for novel

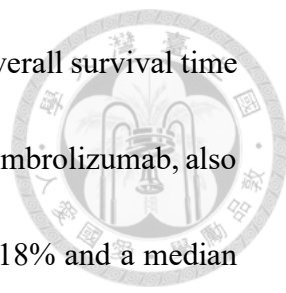
treatments in patients with recurrent or metastatic HNSCC.



1.3 Immune checkpoint inhibitors for HNSCC

Cancer cells survive through several mechanisms, including the avoidance of destruction by the immune system [14]. Immune checkpoints are cell surface receptors that inhibit immune system activation to prevent the development of overwhelming inflammation. However, tumor cells can escape from immune surveillance by expressing immune checkpoint ligands, which activate immune checkpoints to prevent immune activation in the tumor microenvironment. Currently, two checkpoints are widely targeted in the treatment of malignancies: cytotoxic T-lymphocyte-associated protein 4 (CTLA-4) and programmed cell death 1 (PD-1). Ipilimumab, an anti-CTLA-4 antibody, was the first immune checkpoint inhibitor developed and has demonstrated efficacy in patients with metastatic melanoma [15]. In a pooled analysis, more than 20% of patients with melanoma benefited from ipilimumab therapy, resulting in survival longer than 10 years [16], representing the first example of a “clinically cure” for solid cancer using an immunotherapy drug.

Immune checkpoint inhibitors have also been approved for the treatment of cisplatin-resistant recurrent and metastatic HNSCC [17]. In a Phase III trial, nivolumab, an anti-PD-1 monoclonal antibody, showed better efficacy in platinum-refractory HNSCC



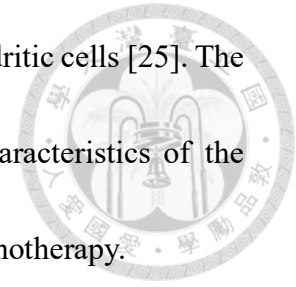
patients, resulting in an overall response rate of 13% and a median overall survival time of 7.5 months (HR: 0.70, $p = 0.01$) [17]. Another anti-PD-1 agent, pembrolizumab, also has good activity against HNSCC, with an overall response rate of 18% and a median overall survival time of 8 months [18]. However, despite these great improvements in cancer immunotherapy for HNSCC treatment, only a small portion of HNSCC patients have a clinical response to therapy. To improve the efficacy of cancer immunotherapies, the mechanisms underlying intrinsic and acquired resistance to anti-PD-1 therapy must be discerned [19]. The tumor microenvironment plays an important role in determining resistance to therapy [20].

1.4 Tumor microenvironment and genomics

1.4.1 Immune cells in the tumor microenvironment

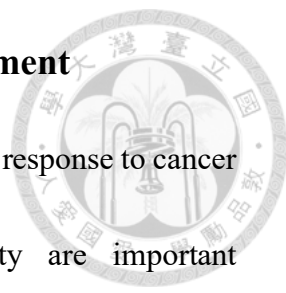
The tumor microenvironment describes the interactions between tumor cells and surrounding cells, structures, and chemicals. In 2014, Tumeh et al. first described that melanoma patient had a good response to anti-PD-1 therapy if the tumor microenvironment had infiltration of CD8⁺ T cells [21]. Since then, several studies have uncovered the composition of “hot” or “inflamed” tumor microenvironments that are associated with a favorable response to cancer immunotherapy [22]. “Inflamed” tumor microenvironments are characterized by CD8⁺ T cell infiltration [21], fewer regulatory

T cells [23], more M1 macrophages [24], and the abundance of dendritic cells [25]. The functions and interactions of immune cells can determine the characteristics of the tumor microenvironment and predict the clinical response to immunotherapy.



Although immune cells in the tumor microenvironment may determine the efficacy of cancer immunotherapy, different immune cells have different contributions to the prognostic impacts across cancer types. CIBERSORT [26] is a bioinformatics database containing information regarding the immune contexts of various cancer types, and analysis revealed that the prognostic roles of immune cells are not universal across all cancer types [27]. For example, memory B cells represent a favorable prognostic factor in lung cancer but are associated with a worse prognosis in breast cancer. In addition, the prognostic effects of some immune cells are not significant. For example, macrophages, which represent the most abundant immune cells found in the tumor microenvironment, do not have a significant prognostic role in all cancer types. This heterogeneity among immune cells may explain the different prognostic roles of different cell types. As an example [28], macrophages can be further classified into two subsets, M1 and M2. M1 macrophages can stimulate immune reactions in the tumor microenvironment. A better understanding of the heterogeneous subsets within our known immune cell classifications will clarify the basic functions of immune cells and their roles in the tumor microenvironment.

1.4.2 Cancer genomics and the tumor microenvironment



The genetic backgrounds of tumors can also predict the clinical response to cancer immunotherapy. Multiple gene mutations and gene instability are important contributors to cancer development. Proteins produced by mutated genes may be recognized as a new antigen and be processed by the antigen presentation machinery as a “neoantigen” on the tumor surface [29]. Therefore, microsatellite instability [30] and a high tumor mutational burden (TMB) [31] are considered to serve as predictive biomarkers for cancer immunotherapy. Apolipoprotein B mRNA editing catalytic polypeptide-like (*APOBEC*) is a gene related to hypermutation in cancer. The induction of *APOBEC* may also results in hypermutation [32].

By contrast, mutations in inflammation-related genes may result in impaired immune functions within the tumor microenvironment. For example, gene alternations associated with the interferon-gamma pathway impairs immune reactions in the tumor [33]. The loss of beta-2 microglobulin [33] also impairs tumor antigen presentation. A functional Wnt/beta-catenin signaling pathway is also crucial for T cell function and differentiation [34]. Therefore, defining the genetic background of individual tumors may be able to predict the tumor response to immunotherapy and allow for adjustments to the treatment strategy for each individual patient.

1.4.3 Lessons from research in the tumor microenvironment:



Finding biomarkers

Biomarkers are important in cancer immunotherapy because they can guide clinicians and patients in selecting the best treatment options and improve understanding of the underlying tumor biology. Various biomarkers have been developed for the purpose of improving cancer therapy strategies. PD-L1, the ligand for PD-1, was first developed to predict responders to PD-1–targeted therapy. PD-L1 was first validated in lung cancer [35]. In patients with HNSCC, higher PD-L1 expression levels predict higher odds of a favorable response. The detection of PD-L1 results in an area under the receiver operating characteristic (ROC) curve (AUC) of approximately 0.65 for predicting good responders [36]. Another biomarker is the interferon-gamma signature, which can be measured using a NanoString-based technique involving a pre-defined profile of barcoded RNA probes [37]. The NanoString interferon-gamma signature has an AUC of approximately 0.75 [36]. These two methods are easily implemented to predict the clinical response to anti–PD-1 therapy. However, the AUCs of these two methods remain unsatisfactory, and the identification of other biomarkers able to predict the clinical response to anti–PD-1 therapy remains essential.

1.4.4 Bioinformatics and multi-omics approaches to human

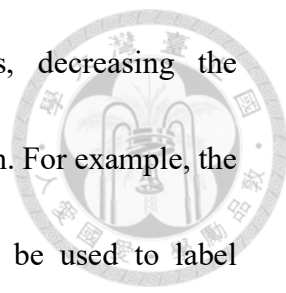
immunology



Some obstacles have limited advances in human cancer immunology research.

First, the genetic background of each human is unique, which can result in broad differences in the biological reactions to stimuli or treatments across cohorts, even with the same cancer type. Therefore, true immunological reactions may be blunted or difficult to be detected in human studies. Second, the genetics of tumors varies from patient to patient and therefore the treatment effect differs. Third, the tumor microenvironment is highly complex, and the types and amounts of the various cell types, cytokines, and chemokines found in the tumor microenvironment and the crosstalk that occurs among these factors may modulate treatment response. Last, the collection of human samples can be difficult, as clinical samples acquired research are typically quite small, which can introduce challenges for multiple types of analyses. Therefore, a new approach to the study of cancer immunology remains necessary.

In recent years, several novel approaches and analytical tools have been developed to decipher the complexity associated with human cancer immunology. In the field of human cancer genomics, rapid next-generation sequencing (NGS) has facilitated our understanding of the individual tumor genetics of each patient [38]. Multiplexed mRNA analysis is also possible to perform in a rapid manner. Several new

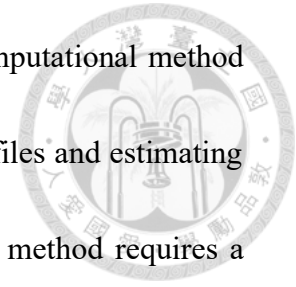


methods have improved the multiplexity of mRNA analyses, decreasing the requirements for specimen quality when performing mRNA research. For example, the NanoString technique, based on mRNA barcoding systems, can be used to label multiple mRNAs in formalin-fixed, paraffin-embedded tissue samples [37]. Cytometry by time-of-flight (CyTOF) is another technique able to analyze multiple targets within a single cell [39]. These methods allow for the application of multiplexed analyses of human immunology.

High-throughput analyses generate large quantities of data that are not easy to analyze. Gene set enrichment analysis [40] is a method for analyzing the significant contributions of pre-specified gene sets, allowing for the investigation of biological pathways that are altered by cancer treatments. Gene sets available for analyses are validated and updated regularly. The gene set analysis method can avoid biased conclusions toward significantly upregulated (or downregulated) genes with unknown biological significance.

Understanding the abundance of certain immune cells in tumors can contribute to determining the significant factors found in the tumor microenvironment that affect the response to therapy. Tissue mRNA analyses can provide multi-omics data analyzing the mRNA expression levels in tumors. However, bulk RNA sequencing represents a mixture of mRNA expression levels across all of the various cell types found in the

tumor and surrounding areas. CIBERSORT [26] is a versatile computational method for quantifying cell fractions from bulk tissue gene expression profiles and estimating the abundance of individual immune cell types in the tissue. The method requires a relatively small amount of tumor tissue for analysis but efficiently estimates the cell composition of interest.

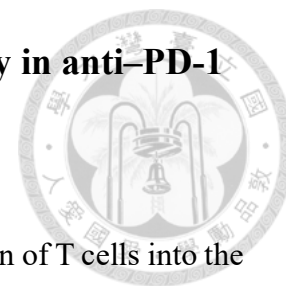


1.5 Anti–PD-1 combination therapy in HNSCC: Rationale and current landscape

1.5.1 Overcoming intrinsic resistance in anti–PD-1 therapy

Anti–PD-1 monotherapy, such as pembrolizumab or nivolumab, is effective in patients with HNSCC [17, 18, 41]. However, modest response rates have been reported in cancer patients due to intrinsic resistance to anti–PD-1 monotherapy [42]. The loss of interferon-gamma (IFN- γ) signaling and impaired antigen presentation are two primary mechanisms underlying this resistance [42]. Overcoming this intrinsic resistance using anti–PD-1-based combination therapy represents a critical approach for improving clinical benefits in HNSCC patients receiving anti–PD-1 therapy.

1.5.2 The role of the antigen presentation machinery in anti-PD-1 therapies

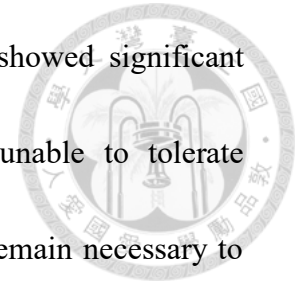


Successful anti-PD-1 therapy induces the increased infiltration of T cells into the tumor environment [21] in response to an adequate antigen-presenting cell niche [43, 44]. Therefore, in situ antigen presentation alone may act as a determining factor for the intrinsic resistance to anti-PD-1 therapy. Current studies have indicated that insufficient IFN- γ signaling [45], low major histocompatibility (MHC) complex expression [46], beta-2-microglobulin (B2M) gene mutation [33], and epidermal growth factor receptor (EGFR) pathway activation [47, 48] are related to impaired antigen processing and presentation. Treatment strategies that augment antigen presentation could be promising approaches for improving anti-PD-1 treatment efficacy.

1.5.3 Anti-PD-1 therapy combined with chemotherapy: Current landscapes and unmet needs

A combination of chemotherapeutic drugs induced immunogenic cell death and enhance antigen presentation in a variety of mouse models [49]. Recent studies have combined chemotherapy with anti-PD-1/PD-L1 therapy in various cancer types, leading to meaningful improvements in survival [41, 50, 51]. In HNSCC, the

combination of pembrolizumab with platinum and fluorouracil showed significant improvements in overall survival [41]. However, in patients unable to tolerate chemotherapy-related toxicity, alternative combination therapies remain necessary to overcome intrinsic resistance to anti-PD-1 immunotherapy. For this reason alone, it is important to uncover and elucidate alternative anti-PD-1 combination regimen to overcome the different mechanisms of intrinsic resistance.

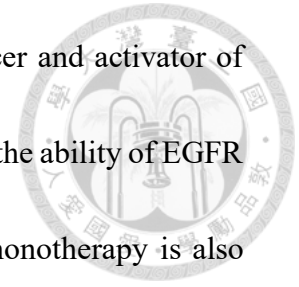


1.6 The role of the EGFR signaling pathway in HNSCC

immunotherapy

EGFR pathway inhibition has been shown to promote antigen presentation and improve immunotherapy efficacy in a pre-clinical model [52]. Lizotte et al. performed a drug screening assay using an ovalbumin (OVA) antigen-specific, H2b-restricted, transgenic CD8⁺ T cell in vitro co-culture system. The study found that EGFR tyrosine kinase inhibitors (TKIs), especially afatinib, increased IFN- γ -induced MHC class I expression in OVA-expressing ID8 tumor cells and enhance tumor cell lysis by OVA-specific transgenic CD8⁺ T cells[52]. In a syngeneic mouse model using MC38 colon cancer cell lines in C57BL/6J mice, adding afatinib to anti-PD-1 treatment suppressed tumor growth [52]. Another study showed that EGFR-TKIs augment anti-PD-1 effectiveness by increasing human leukocyte antigen (HLA) expression and

downregulating PD-L1 via the Janus kinase (JAK)/signal transducer and activator of transcription (STAT) pathway [47, 48]. These studies demonstrated the ability of EGFR inhibition to enhance antigen presentation. In addition, afatinib monotherapy is also proved to improve the objective response rate (ORR) and progression-free survival (PFS) rate in recurrent or metastatic HNSCC [53, 54]. These data indicate the ability of EGFR-TKIs to augment antigen presentation and tumor suppression, and therefore raise the potential efficacy of combination anti-PD-1 and EGFR-TKIs for cancer immunotherapy.



Chapter 2 Hypothesis and specific aims



2.1 Hypothesis

This study tested the hypothesis that adding afatinib, an EGFR-TKI, can improve the treatment efficacy of anti-PD-1 therapy in patients with HNSCC by augmenting the antigen presentation machinery.

2.2 Specific aims

To test this hypothesis, this study proposed the following specific aims:

1. Examine the efficacy (objective response rate and survival) of afatinib plus pembrolizumab in patients with HNSCC.
2. Determine the biological effects on the tumor microenvironment due to the combination of afatinib plus pembrolizumab in patients with HNSCC.
3. Examine whether any genetic signatures can predict the clinical response to combination afatinib plus pembrolizumab therapy.
4. Examine whether the heterogeneity of immune cells in the tumor microenvironment can predict treatment response.

Chapter 3 Materials and methods



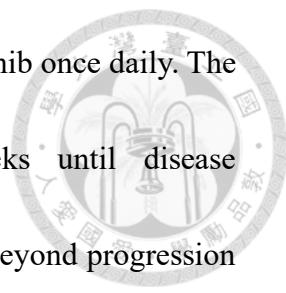
3.1 Clinical trials

3.1.1 Study approval

This study protocol was approved by the Institutional Review Board of the National Taiwan University Hospital and is registered with ClinicalTrials.gov (NCT03695510).

3.1.2 Study design

This study was designed as a single-arm, Phase II trial with Simon's 2-stage design. The key eligibility criteria for inclusion in the study were: 1) HNSCC diagnosis; 2) platinum-refractory, which was defined as tumor progression or recurrence within 6 months after the last dose of platinum-based therapy administered as adjuvant therapy, or disease progression after taking platinum-based therapy for recurrent or metastatic disease; 3) Response Evaluation Criteria in Solid Tumors (RECIST) 1.1-measurable lesions; 4) Eastern Cooperative Oncology Group (ECOG) performance score of 0 or 1; 5) acceptable bone marrow, hepatic, and renal functions; and 6) negative hepatitis B virus surface antigen, negative anti-hepatitis C virus, and negative anti-human immunodeficiency virus (HIV). The study treatment protocol was 200 mg

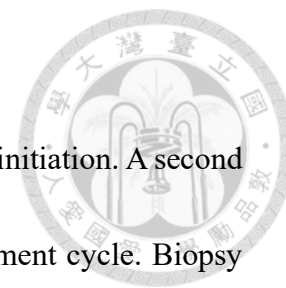


pembrolizumab once every three weeks combined with 40 mg afatinib once daily. The study administered afatinib–pembrolizumab every three weeks until disease progression, intolerable toxicity, or patient withdrawal. Treatment beyond progression was allowed if pseudoprogression was suspected. Afatinib dose titration for treatment-related toxicity was allowed, but no dose titration for pembrolizumab was permitted. The trial assessed tumor response every nine weeks during the first 18 weeks and every 12 weeks after that. Tumors were assessed and analyzed using computed tomography or magnetic resonance imaging.

3.1.3 Efficacy assessment

The primary endpoint was the best ORR, according to RECIST 1.1 criteria. The secondary endpoints were PFS, overall survival (OS), and duration of response (DoR). PFS was calculated from the day of first dosing to disease progression, intolerable toxicity, or death. Patients who did not have disease progression were censored on the last day of tumor evaluation. OS was calculated from the day of dosing to the day of death. For survivors, the data were censored on the last day of known survival status. For responders, DoR was calculated from the day of partial response to the day of disease progression or death. Patients who did not have disease progression were censored on the last day of tumor evaluation.

3.1.4 mRNA expression analysis



Each eligible patient was subjected to biopsy before treatment initiation. A second post-treatment tumor biopsy was obtained prior to the fourth treatment cycle. Biopsy samples were fixed in formalin for all downstream analyses. Gene expression was measured using RNA isolated from formalin-fixed paraffin-embedded (FFPE) biopsy tissue using NanoString technology. Total RNA was isolated and purified using a Qiagen RNeasy FFPE kit (Qiagen, Valencia, CA, USA), following the manufacturer's instructions. Extracted mRNA was analyzed using an nCounter PanCancer Immune Profiling Panel (NanoString Technologies, USA), as described previously [37]. Digital data acquisition via the nCounter Digital Analyzer (NanoString Technologies) was performed by Cold Spring Biotech Corporation (Taipei, Taiwan). nSolver 4.0 Analysis Software (NanoString Technologies, USA) and R 3.5.0 were used for data analysis. Linear normalization of mRNA expression data was generated by nSolver 4.0. In the gene differential expression analysis, an adjusted p-value was calculated using the Benjamini-Yekutieli method in nSolver 4.0 software. Gene Set Enrichment Analysis (GSEA) v4.1.0 (Broad Institute, MA, USA) and GSEA Preranked v.7.2 (Broad Institute, MA, USA) were used for enrichment analysis [40]. Kyoto Encyclopedia of Genes and Genomes (KEGG) and Gene Ontology (GO) datasets were retrieved from MSigDB v7.4 (<https://www.gsea-msigdb.org/gsea/msigdb/>). Gene sets with nominal p-values <

0.05 and false discovery rate (FDR) q values < 0.1 were selected for further analysis.

Cytoscape v3.8.2 (National Institute of General Medical Sciences, MD, USA) [55],

EnrichmentMap v3.3.2 (University of Toronto, Canada) [56], and StringApp v1.6.0

(University of California, San Francisco, CA, and University of Copenhagen, Denmark)

[57] were used for analysis. CIBERSORTx (Stanford University, CA) and LM22 gene

signatures for immune cell enumeration were used for immune cell profiling analysis

[26].

3.1.5 Comprehensive genomic profiling

Pre-treatment tumor biopsies or archival tumor tissues were used for comprehensive genomic profiling. Biopsy collection after disease progression was

performed only with patients' consent. FFPE samples were transported to Foundation

Medicine (Cambridge, MA) and analyzed using a FoundationOne CDx Panel. The

methods applied in the current study for next-generation sequencing-based genomic

assays have previously been validated and reported [38]. The current assay interrogated

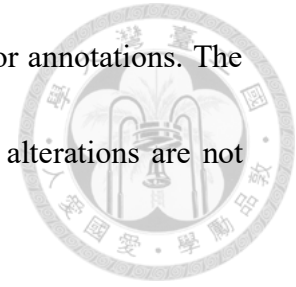
324 genes and the introns of 36 genes known to be involved in gene rearrangements.

Copy number amplification cutoffs for the present study were defined as four copies of

ERBB2 and six copies of all other genes. The mutation allele frequency (MAF) results

were provided by Foundation Medicine on request. The results from all patients were

summarized and visualized in Microsoft Excel using different color annotations. The results for equivocal amplification, equivocal loss, and subclonal alterations are not presented in the figures included here.



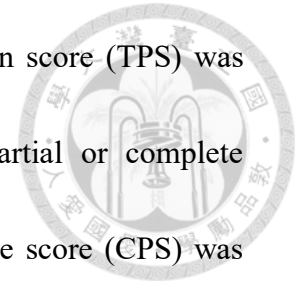
3.1.6 TCGA HNSCC data acquisition and analysis

To confirm the roles played by specific genetic alterations and their impacts on the tumor microenvironment, The Cancer Genome Atlas (TCGA) HNSCC PanCancer Atlas [58] database was analyzed using cBioPortal (<https://www.cbioportal.org/>). A gene of interest was used to query the database, and differential mRNA expression levels between groups according to gene status (gene alteration vs. wild-type) were obtained from the “mRNA” module of the “Comparison/Survival” tool in cBioPortal. The differential mRNA expression data were then ranked according to the value of the log of the ratio of mRNA differential expression. For enrichment analysis, the ranked mRNA data were analyzed using GSEA Preranked v.7.2 (Broad Institute, MA, USA).

3.1.7 PD-L1 testing

PD-L1 immunohistochemistry (IHC) was performed using anti-PD-L1 antibody 22C3 clone (Dako, US) and the Dako automated platform (Dako, US) at the Department of Pathology, National Taiwan University Hospital. All PD-L1 scoring was performed

by a single pathologist (Huang YL). The PD-L1 tumor proportion score (TPS) was calculated as the percentage of viable tumor cells showing partial or complete membrane staining at any intensity. The PD-L1 combined positive score (CPS) was calculated as the number of PD-L1–stained cells (tumor cells, lymphocytes, and macrophages) divided by the total number of viable tumor cells, multiplied by 100. At least 100 viable cancer cells were evaluated in each sample [59].



3.1.8 Statistical analysis

This study was performed as a single-arm, Phase II trial, and the primary endpoint was the best ORR based on Simon’s 2-stage design. The null hypothesis that the true response rate is 15% will be tested against a one-sided alternative. During the first stage, 13 patients were recruited, and the study would have been stopped if two or fewer responses were observed among these 13 patients. During the second stage, 16 additional patients were recruited, resulting in a total of 29 patients. The null hypothesis was rejected if eight or more responses were observed among all 29 patients. This design yields a type I error rate of 0.05 (one-sided) and a power of 0.9 when the true response rate is 40%. Survival estimates were performed using Kaplan–Meier survival analyses and log-rank Cox proportional analyses. MedCalc Statistical Software version 19.7 (MedCalc Software Ltd, Ostend, Belgium), GraphPad Prism version 9.0.2

(GraphPad Software, LCC. San Diego, US), and Microsoft Office 365 were used to perform data analyses and figure generation.



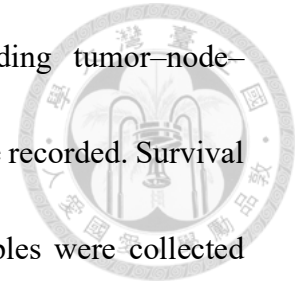
3.2 Deciphering the tumor microenvironment in HNSCC

3.2.1 Patient population and specimen collection

We enrolled patients with oral squamous cell carcinoma (OSCC) in this study. Informed consent was obtained from each patient before performing the operation. Patients with a pathological diagnosis of OSCC were enrolled. All patients underwent total surgical excision of OSCC lesions at the National Taiwan University Hospital (NTUH). Patients receiving induction chemotherapy or neoadjuvant chemoradiation and patients with recurrent or second HNSCC were excluded. The treatment for OSCC was guided by the current treatment protocols in place at NTUH. OSCC specimens were obtained from the complete surgical excision of lesions from the buccal region, tongue, gingival areas, soft palate, or floor of the mouth. If patients had two or more clinically positive lymph node metastases, lymph nodes were also removed for analysis. This study was reviewed and approved by the Human Investigation Review Committee at NTUH.

Details of the patients' oral habits, including daily/weekly consumption of cigarettes, alcohols, and areca nuts (*Areca catechu*) chewing, as well as the duration of

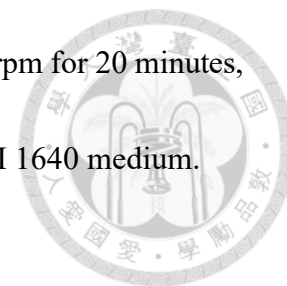
these habits, were recorded. Other clinical parameters, including tumor–node–metastasis (TNM) stage, comorbidities, and treatment courses, were recorded. Survival status was recorded for analysis. Patients' blood and tumor samples were collected during the operation.



3.2.2 Isolation of peripheral blood mononuclear cells and T cells

Surgical specimens and peripheral blood were collected from each patient during the operation. Blood samples were centrifuged at 1200 rpm for 10 minutes to remove platelets. The remaining samples were diluted with an equal volume of Hank's balanced salt solution, and peripheral blood mononuclear cells (PBMCs) were enriched by Ficoll-Paque PLUS. After centrifugation at 3000 rpm for 20 minutes, the intermediate layer of cells was collected and washed with RPMI 1640 medium. PBMCs were counted for subsequent surface or intracellular staining. Cells were cultured in RPMI 1640 medium supplemented with 10% certified fetal bovine serum (FBS), 100 U/mL penicillin, 100 µg/mL streptomycin, 2 mM L-glutamine, 100 mM HEPES, 100 µM 2-mercaptoethanol, 1% MEM vitamin, and 1% MEM non-essential amino acids. Peripheral blood CD4⁺ T cells were purified by RosetteSep™ Human CD4⁺ T Cell Enrichment Cocktail. After a 2- minutes reaction at room temperature, whole blood was diluted with phosphate-buffered saline (PBS) containing 4% FBS, and CD4⁺ T cells

were enriched by Ficoll-Paque PLUS. After centrifugation at 3000 rpm for 20 minutes, the intermediate layer of cells was collected and washed with RPMI 1640 medium.

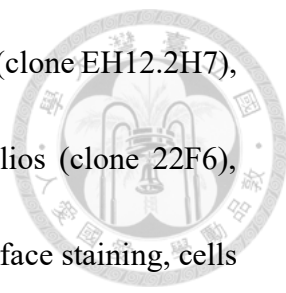


3.2.3 Isolation of tumor-infiltrating lymphocytes

The specimens collected during surgery were mechanically disrupted in a 10-cm dish containing 2–3 mL culture medium. Tumor cell suspensions were filtered through a 40- μ m filter, and the cells were enriched by Ficoll-Paque PLUS. The tumor tissue mass suspension was gently passed through a 400- μ m sieve (Sigma-Aldrich), followed by filtration using 100- μ m and 40- μ m filters, and tumor-infiltrating lymphocytes (TILs) were enriched by Ficoll-Paque PLUS. Cell numbers were counted for subsequent surface or intracellular staining. If required, TILs were further enriched using a discontinuous Percoll gradient (25%, 55%, and 100%).

3.2.4 FACS staining and analysis

The following fluorochrome-conjugated monoclonal antibodies (mAbs) were used for fluorescent-assisted cell sorting (FACS) experiments: anti-CD4 (clone RPA-T4), anti-CD25 (clone M-A251), anti-CD127 (clone eBioRDR5), anti-CCR6 (clone G034E3), anti-CD45RA (clone HI100), anti-CCR7 (clone G043H7), anti-ICOS (clone ISA-3), anti-HLA-DR (clone L243), anti-CD161 (clone HP-3G10), anti-CD38 (clone



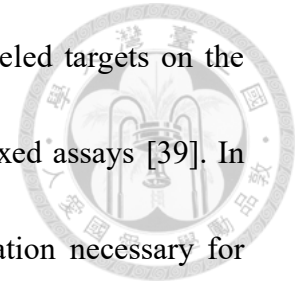
HB7), anti-CD39 (clone A1), anti-CD31 (clone WM-59), anti-PD-1 (clone EH12.2H7), anti-FOXP3 (clone PCH101), anti-CTLA4 (clone 14D3), anti-Helios (clone 22F6), anti-IL10 (clone JES3-9D7), and anti-Ki-67 (clone 20Raj1). For surface staining, cells were stained with fluorochrome-labeled mAbs for 30 min at 4°C in 100 µL staining buffer (PBS containing 4% FBS). Appropriate isotype antibody controls were used for each sample. For intracellular staining, cells were surface stained and subsequently fixed and permeabilized using the Fixation/Permeabilization Kit (eBioscience) or Cytofix/Cytoperm™ Kit (BD Biosciences), following the manufacturer's instructions. For intracellular cytokine analysis, cells were stimulated with phorbol 12-myristate 13-acetate (PMA; 10 ng/mL; Sigma-Aldrich) and ionomycin (1 µg/mL; Sigma-Aldrich) in the presence of monensin (2 µM; eBioscience) for 4 hours prior to surface staining and fixation.

Flow cytometric analysis was performed on a FACSCanto II or an LSRFortessa flow cytometer (BD Biosciences). Data were exported as FCS 3.0 for further analysis in FlowJo software (Tree Star).

3.2.5 Flow cytometry using mass cytometry

The small quantity of immune cells tumor specimens makes multiplexed experiments and assays using traditional flow cytometry difficult to perform. Cytometry by time-of-flight (CyTOF) is a novel form of mass cytometry using isotype-

labeling antibodies that can be applied to detect and quantify labeled targets on the surfaces and interiors of single cells, allowing for highly multiplexed assays [39]. In CyTOF analysis, the difficult and complicated spectral compensation necessary for flow cytometry is not required. The analyses in this study were accomplished using a CyTOF 2 instrument (Fluidigm Corporation) through a service provided by the Genomics Research Center Mass Spectrometry Facility (Genomics Research Center, Academia Sinica).



Chapter 4 Results



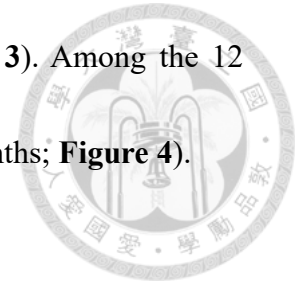
4.1 Clinical studies

In total, 29 patients were enrolled in the study from January 2019 to March 2020. The cutoff for data analysis was February 11, 2021. The median follow-up of the study was 20.1 months. Patient characteristics are summarized in Table 1. One patient discontinued treatment for personal reasons, and one patient discontinued therapy due to decreasing functional status.

4.1.1 Afatinib plus pembrolizumab therapy showed improved efficacy in HNSCC patients

During the first stage, 7 of 13 patients responded to therapy (ORR: 53.8% [95% confidence interval (CI): 25.1%–80.8%]). The response rate met the pre-specified criteria, and the study progressed to the second stage. Overall, one patient had a complete response, and eleven patients had confirmed partial response (ORR: 12/29, 41.4% [95% CI: 23.5%–61.1%]; **Figure 1**). The ORR result met the primary endpoint of the study. Stable disease during therapy was registered for 7 of 29 patients (24.1% [95% CI: 10.3%–43.5%]). The overall disease control rate was 65.5% (95% CI: 45.7%–82.1%). The median PFS was 4.1 months (95% CI: 1.9–6.3 months; **Figure 2**), and the

median OS was 8.4 months (95% CI: 4.1–10.8 months; **Figure 3**). Among the 12 responders, the median DoR was 4.9 months (95% CI: 2.0–7.9 months; **Figure 4**).



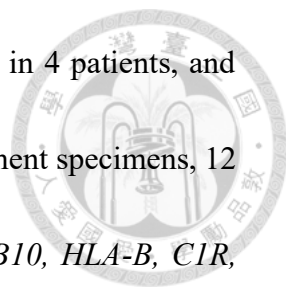
4.1.2 The toxicities associated with afatinib plus pembrolizumab therapy were tolerable

All patients (100%) experienced at least one treatment-related toxicity event, and 11 (37.9%) patients experienced Grade 3 or higher treatment-related toxicity events (Table 2). Twelve patients (41.4%) experienced afatinib dose reduction due to toxicity. One patient discontinued afatinib due to Grade 2 pneumonitis. One patient expired due to a carotid blow-out. One patient committed suicide. One patient with a history of ischemic stroke and stable atrial fibrillation was found dead at home, and the cause of death was determined to be cardiovascular disease.

4.1.3 Biomarker analysis

4.1.3.1 mRNA expression analysis in paired biopsy tissues showed that afatinib plus pembrolizumab treatment augments antigen presentation machinery

Specimens from 9 patients with adequate paired pre- and post-treatment biopsy tissues were analyzed for mRNA expression (**Figure 5**). The best response recorded for



these 9 patients were: partial response in 3 patients, stable disease in 4 patients, and disease progression in 2 patients. By comparing pre- and post-treatment specimens, 12 genes (*CXCL13*, *CXCL9*, *CFB*, *LAG3*, *CD7*, *CD3D*, *CD8A*, *PSMB10*, *HLA-B*, *C1R*, *HLA-A*, and *FLT3LG*; **Figure 6**) were found to be significantly upregulated after treatment, whereas 14 genes (*RRAD*, *CCL20*, *IL1RN*, *FN1*, *IL1RL1*, *CD24*, *ANXA1*, *EGR1*, *THBS1*, *TNFRSF12A*, *LRP1*, *BCL2L1*, *TNFRSF10B*, and *MAP2K1*; **Figure 7**) were significantly downregulated after treatment. Gene network analysis of the 12 upregulated genes using StringApp showed that *HLA-A*, *HLA-B*, *CD8A*, and *CD3E* were core genes affected by combination therapy (**Figure 8**).

We analyzed the data by CIBERSORT to identify changes in immune cell abundance within the tumor microenvironment comparing before and after treatment. In the KEGG GSEA analysis, 11 gene sets were found to be upregulated (nominal $p < 0.05$, FDR $q < 0.1$) after afatinib–pembrolizumab treatment, which were involved in antigen processing and presentation, natural killer (NK) cell–mediated cytotoxicity, endocytosis, autoimmunity, and inflammation (**Figure 12**). In line with the KEGG analysis results, the GO Biological Process GSEA analysis (**Figure 12**) also identified the upregulation of antigen processing and presentation and NK cell–mediated cytotoxicity pathways after treatment. Other upregulated gene sets included genes involved in the adaptive immune response, T cell chemotaxis, T cell selection, and

leukocyte-mediated toxicity (nominal $p < 0.05$, FDR $q < 0.1$). Three gene sets associated with tolerance induction and negative leukocyte and lymphocyte regulatory function were also upregulated after treatment. Leading-edge analysis revealed that *FOXP3* was at the leading edge of all three upregulated gene sets (

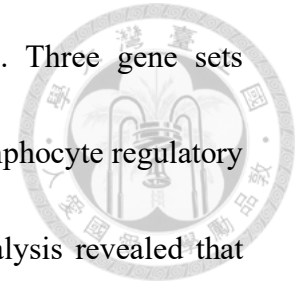
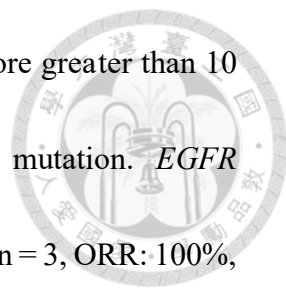


Figure 13). Afatinib–pembrolizumab treatment significantly downregulated 194 gene sets (nominal $p < 0.05$, FDR $q < 0.1$). In an enrichment map analysis, the majority of downregulated gene sets were found to be closely related. The top 10 downregulated gene sets were associated with cell differentiation, generation, and proliferation (**Figure 12**). Gene sets related to IFN- γ and IFN- α function did not show significant changes in this analysis (GOBP interferon gamma mediated signaling pathway: normalized enrichment score (NES): 1.42, $p = 0.051$, $q = 0.34$; GOBP interferon alpha production: NES: -0.76 , $p = 0.85$, $q = 0.919$). We used CIBERSORTx to analyze changes in the abundance of immune cells comparing before and after treatment, which showed no significant changes (**Figure 9, Figure 10, Figure 11**).

4.1.3.2 Targeted gene sequencing analysis revealed that unaltered methyl-thioadenosine phosphorylase could serve as a potential biomarker for response to therapy

Twenty-five patients (86.2%) had fresh or archival tissues available for analysis

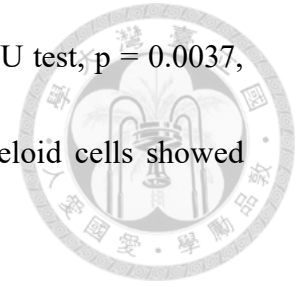


(**Figure 14**). No patients had a tumor mutational burden (TMB) score greater than 10 mutations/megabase. No patients had a known *EGFR* driver mutation. *EGFR* amplification predicted a higher response rate (*EGFR* amplification: n = 3, ORR: 100%, Fisher's exact test: p = 0.07). Methyl-thioadenosine phosphorylase (*MTAP*) loss or mutation predicted a lower response rate (*MTAP* loss or mutation, n = 5, ORR: 0%, Fisher's exact test: p = 0.046). Patients with *MTAP* loss or mutation had a shorter PFS (with loss or mutation, PFS median: 1.9 months [95% CI: 0.7–4.1 months] vs. without loss or mutation, PFS median 5.5 months [95% CI: 2.0–7.0 months]; hazard ratio [HR]: 4.2 [95% CI, 1.3–13.3], p = 0.014) (**Figure 15**) and shorter OS (with loss or mutation, OS median: 3.8 months [95% CI: 2.3–8.4 months] vs. without loss or mutation, OS median 9.0 months [95% CI: 5.6–13.0 months]; HR: 4.2 [95% CI, 1.3–13.4], p = 0.015; **Figure 16**).

4.1.3.3 GSEA analysis using study data and TCGA data showed that tumors with unaltered MTAP presented an inflamed microenvironment

KEGG enrichment analysis comparing *MTAP* loss/mutation (altered *MTAP*, n = 5) with *MTAP* wild-type (unaltered *MTAP*, n = 15) showed the downregulation of the Toll-like receptor signaling pathway and the JAK-STAT signaling pathway (**Figure 17**). Compared with tumors featuring altered *MTAP*, tumors with unaltered *MTAP* had more

abundant CD8⁺ T cells in the microenvironment. (Mann–Whitney U test, $p = 0.0037$, FDR $q = 0.08$; **Figure 18**). No other subsets of lymphoid or myeloid cells showed significant differences in this analysis (**Figure 19, Figure 20**).

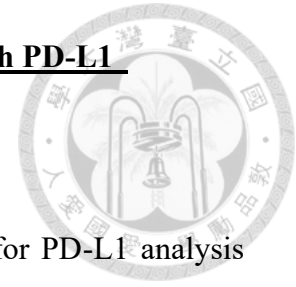


To confirm the role of *MTAP* alternation in the HNSCC tumor microenvironment, we analyzed 523 patients/samples from the TCGA HNSCC database. Eighty (15%) patients had *MTAP* gene alterations, and the majority of these (75 patients, 93.75%) had *MTAP* deep deletion. KEGG and GO enrichment analyses of 19,874 mRNA genes revealed that immune response-related gene sets were significantly downregulated in HNSCC patients with *MTAP* alterations (**Figure 17**).

4.1.3.4 Post-progression, targeted gene sequence analysis revealed acquired loss of *MTAP* in a patient with disease progression after initial response

Three patients had paired pre-treatment and post-progression biopsy tissues for targeted gene sequence analyses. The heterogeneous responses of clones were noted for two patients (**Figure 21**). One patient had a new *MTAP* loss in the post-treatment tissue. Two patients each had a new *INPP4B* mutation. One *JAK1* in one patient and one *JAK3* missense mutation in one patient were detected.

4.1.3.5 A high response rate is observed in patients with high PD-L1 expression



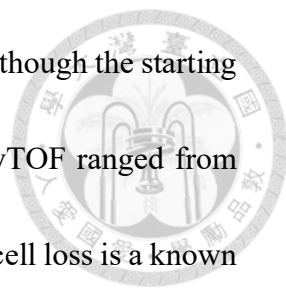
Twenty-eight (96.6%) patients had adequate tissue samples for PD-L1 analysis (Table 1). For patients with high PD-L1 expression, the ORR was numerically but not statistically higher than for patients with low PD-L1 expression (PD-L1 TPS \geq 50, ORR: 71% vs. TPS < 50, ORR: 33%, Fisher's exact test: $p = 0.1$; PD-L1 CPS \geq 20, ORR: 63% vs. CPS < 20, ORR: 35%, Fisher's exact test: $p = 0.23$).

4.2 Microenvironment study using a multiplexed proteomics approach

4.2.1 Pilot experiment using CyTOF and trouble-shooting

To test whether the CyTOF machine at Sinica is able to perform our desired analyses, a pilot experiment was performed using the Maxpar® Human Helper T Cell Phenotype Panel Kit. The standard Maxpar staining protocol is designed for staining three million cells. In our study setting, only one million PBMCs were collected, and samples were labeled using antibodies at 1/3 or 2/3 the recommended concentration to examine TIL distributions.

As shown in **Figure 22A**, no differences in CD4 or CD3 signal intensity were observed across staining conditions, suggesting that the decreased antibody



concentrations tested were sufficient to stain one million PBMCs. Although the starting cell number was one million cells, the total events acquired by CyTOF ranged from 3000 to 9000, and the DNA⁺ events ranged from 900 to 3000. First, cell loss is a known consequence of CyTOF acquisition, with an average recovery rate of approximately 20%. Second, according to the CyTOF technician at Sinica, only 10%–40% of the total sample was acquired and recorded due to the limited input sample volume of the CyTOF machine. Third, the recommended centrifugation speed ($300 \times g$) may be too low to pellet all cells during the staining procedure. To resolve the issue of cell loss, we consulted a specialist at the Fluidigm Corporation, and the only solution identified was to increase the starting cell number because cell loss in the CyTOF2 machine cannot be circumvented. To account for limited sample acquisition during a single CyTOF run, we combined data acquired during different runs. To collect more cells for the staining procedure, we increased the centrifugation speed to $4000 \times g$, a speed that is regularly used for flow cytometry staining in Dr. Chia's lab. To validate the CyTOF data, we examine the marker expression patterns in CD4⁺ T cells. **Figure 22B** shows that CD45RA and CD45RO expression was mutually exclusive, and CD25^{hi} cells, which characterize Treg cells, lack CD127 expression. These findings indicate that the data collected by CyTOF is credible.

To analyze the massive amounts of high-dimensional data acquired by CyTOF

analyses, t-distributed stochastic neighbor embedding (t-SNE) tools are widely used.

Figure 23A shows the expression of individual markers on a t-SNE map. CD4⁺ and CD8⁺ T cells can easily be identified. We manually grouped the cells into five populations. Populations 1 and 3 were CD4⁺ and CD8⁺ T cells, respectively (**Figure 23B**). Treg cells, which express high CD25 but low CD127 levels, can also be identified in the lower left region of the CD4⁺ T cell population. Population 2 expresses CD3 and CD8 but was not clustered with Population 3. Different from Population 3, Population 2 also expressed CD161 and CCR5. Because both CD161 and CCR5 are highly expressed on natural killer T (NKT) cells, we characterized Population 2 as NKT cells. Although we did not stain B cell markers, Population 4 could represent B cells due to high CD45RA, CCR6, and CXCR5 expression.

In addition to t-SNE analyses, spanning-tree progression analysis of density-normalized events (SPADE) analysis is commonly used to perform unbiased analyses. Similar to t-SNE analysis, SPADE groups cell populations according to differential expression patterns (**Figure 24**).

The Cell-ID 20-Plex Pd Barcoding Kit was used to label samples with various combinations of metal-tagged antibodies. The labeled samples can be pooled into a single tube for the subsequent staining and data acquisition. During data analysis, different samples can be separated according to the unique barcodes. This procedure

can be used to compare PBMCs and TILs in samples collected from patients. We stained PBMCs from three individuals using the Pb Barcoding sample codes 1, 2, and 3 (**Figure 25A**). As expected, a 108Pb signal was detected in $105\text{Pd}^-106\text{Pb}^-$ but not $105\text{Pd}^+106\text{Pd}^-$ or $105\text{Pd}^-106\text{Pd}^+$ populations (**Figure 25B**), suggesting that the barcoding system can be used for our analyses.

After overcoming the issues associated with low event acquisition, we were able to collect more than 30,000 events from each sample. To further test whether t-SNE analysis can be used to identify T helper cell subsets, as suggested by Fluidigm, we analyzed $\text{CD4}^+\text{CD3}^+$ T cells using t-SNE tools. According to the distinct phenotypes identified in the t-SNE analysis (**Figure 26A**), six T helper cell subsets can be defined (**Figure 26B**).

In our project, we aimed to explore the expression patterns of chemokine receptors on immune cells obtained from PBMCs and TILs. We designed a multi-marker panel, including cell identity markers, most of the chemokine receptors expressed by immune cells, and inhibitory receptors involved in immunosuppression (**Figure 27A**). Using this panel, we are able to uncover the atlas of chemokine and inhibitory receptor landscapes among CD4^+ T cells, CD8^+ T cells, NK cells, B cells, monocytes, macrophages, DCs, and pDCs (**Figure 27B**). Furthermore, we are able to further subdivide cells into naïve and memory subsets by co-staining with CD45RA, CD27,

CD127, and HLA-DR.



4.2.2 CyTOF study using cancer patient tissues

Previous tests confirmed the feasibility of applying CyTOF analyses to study cancer immunology in HNSCC. Therefore, we applied CyTOF to the analysis of TILs and PBMCs collected from cancer patients.

4.2.2.1 Differences in CD3⁺ T cells between PBMCs and TILs

In PBMCs (**Figure 28**), more cells were identified as CD45RA⁺ and CCR7⁺, which reflects the naïve nature of PBMCs. In TILs (**Figure 29**), the expression levels of CD45RA and CCR7 were low, indicating that most T cells in TILs were memory T cells or activated T cells.

In both PBMCs and TILs, PD-1 is the predominant checkpoint expressed on immune cells. CTLA-4 and TIM-3 were also detected, but the frequencies were low. The frequency of PD-1 expression was higher in TILs than in PBMCs. In the cluster analysis, PD-1⁺ T cells were distributed widely across the t-SNE map, indicating the heterogeneity of PD-1⁺ T cells in TILs. Exhausted T cells identified in TILs from patients with HNSCC were typically PD-1⁺. CTLA-4⁺ T cells were also identified among PD-1⁺ T cells, especially among the CD4⁺ T cells. TIM-3⁺ T cells were not very

abundant among the TILs from patients with HNSCC.

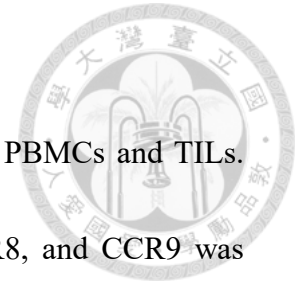
The chemokine receptor landscape is also different between PBMCs and TILs.

The expression of CXCR3, CXCR4, CCR5, CCR6, CCR7, CCR8, and CCR9 was

frequently detected in both PBMCs and TILs. However, in PBMCs, most PD-1⁺ T cells

displayed the low expression of chemokine receptors. In the tumor microenvironment,

chemokine receptor–positive T cells were typically also PD-1⁺.



Chapter 5 Discussion

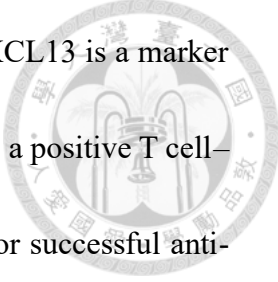


- **Afatinib plus pembrolizumab therapy is an effective option for patients with HNSCC**

This study explored the effects of EGFR-TKI treatment combined with anti-PD-1 therapy in platinum-refractory HNSCC patients. The study met the primary endpoint of ORR, with manageable toxicities in HNSCC patients. In the biomarker analyses, we also identified several potential predictive therapeutic biomarkers, including high PD-L1 expression, *EGFR* amplification, and unaltered *MTAP*. Further studies in larger sample sizes are warranted to confirm the efficacy of this therapeutic strategy and the roles of these biomarkers in this population.

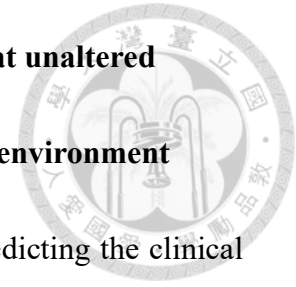
- **Multi-omics analysis of paired tissue samples revealed the upregulation of antigen presentation machinery and the stimulation of immune functions in the tumor microenvironment**

By using paired human tissue mRNA analyses, we identified that genes involved in antigen processing and presentation signaling pathways, such as *HLA-A*, *HLA-B*, and *PSMB10*, were significantly upregulated in post-treatment specimens. In line with previous reports on anti-PD-1 treatment, we also identified the upregulation of



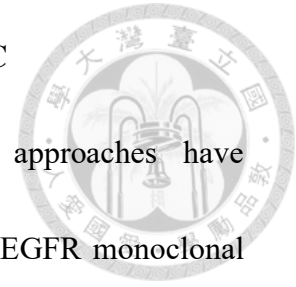
CXCL13, *CXCL9*, and *FLT3LG* in post-treatment biopsy tissues. *CXCL13* is a marker of T cells that are preferentially reactive to neoantigens and serves as a positive T cell–intrinsic marker of anti–PD-1 sensitivity [60]. *CXCL9* is required for successful anti-tumor responses following PD-1 blockade in an IFN- γ –dependent manner [61]. *FLT3LG* has been shown to stimulate dendritic cell maturation and is correlated with the abundance of intra-tumoral stimulatory dendritic cells [62]. On the other hand, this combination therapy approach resulted in the downregulation of several key suppressive genes involved in immune reactivity. *CCL20*, a ligand for *CCR6*, has been shown to chemoattract *CCR6*⁺ regulatory T cells, which have higher tumor-suppressive activity compared with other T cells [63]. *CD24* is a “don’t eat me” signal that can inhibit macrophage function via *Siglec-10* [64]. The downregulation of these genes suggests a less immunosuppressive tumor environment. In the gene set analyses, pathways involving inflammation, NK cell–mediated cytotoxicity, the adaptive immune response, and endocytosis were also found to be upregulated. In addition to immune-related pathways, pathways related to tumor growth were also significantly suppressed. These results provide positive evidence that the afatinib–pembrolizumab therapeutic regimen was involved in reprogramming the tumor environment, possibly through augmented antigen presentation and immune responses, resulting in suppressed tumor growth.

- **Genetics studies and post-progression biopsies revealed that unaltered MTAP may regulate immune functions in the tumor microenvironment**



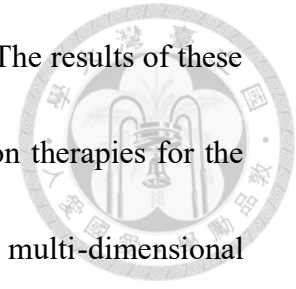
In this study, *MTAP* was identified as a potential gene for predicting the clinical benefits of anti-PD-1-based immunotherapy. *MTAP* is an enzyme that catalyzes the breakdown of methyl-thioadenosine (MTA) in the cell. The loss of *MTAP* function may interfere with *STAT1* function, inhibiting IFN-mediated gene functions [65]. In a report analyzing ipilimumab monotherapy in melanoma patients, the loss of IFN- γ pathway genes, including *MTAP*, predicted a poor response to ipilimumab [66]. In this study, patients with *MTAP* alterations showed worse ORR and prognosis. Tumors with *MTAP* alterations contained fewer CD8⁺ T cells in the microenvironment. In the GSEA, tumors with *MTAP* loss or mutation showed the downregulation of Toll-like receptor and JAK-*STAT* signaling pathway components. We also identified one patient with a new *MTAP* loss in the post-progression biopsy specimen. Our analysis using TCGA HNSCC database (Figure 3D) also supported the findings that patients with *MTAP* alterations were associated with suppressed immune reaction factors in the tumor microenvironment. These findings suggested a role for *MTAP* in HNSCC cancer immunotherapy, and the contributions of *MTAP* to cancer immunotherapy warrants further research.

- **The outlook for anti-PD-1 combination therapy in HNSCC**



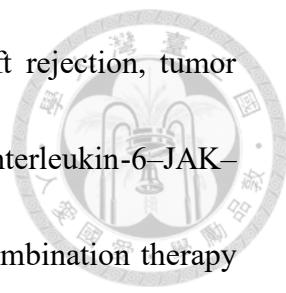
Several anti-PD-1/PD-L1-based combination therapeutic approaches have reported positive outcomes in HNSCC trials. Cetuximab, an anti-EGFR monoclonal antibody, was combined with pembrolizumab in HNSCC patients. The Phase II study also showed an encouraging ORR of 45% [67], highlighting the importance of EGFR inhibition combined with anti-PD-1 therapy in HNSCC. Lenvatinib, a multitarget TKI, was combined with pembrolizumab in HNSCC [68], and the preliminary Phase I/II results showed that the combination treatment resulted in an improved ORR of 46% and an improved PFS of 4.7 months. A confirmatory Phase III trial is ongoing examining this combination approach as a first-line treatment option for HNSCC patients. Anti-PD-1 combination therapy using the CTLA-4 antibody ipilimumab demonstrated efficacy in melanoma [69], renal cell carcinoma [70], and non-small cell lung cancer (NSCLC) [71]. Tremelimumab, another CTLA-4 antibody, was combined with durvalumab, an anti-PD-L1 antibody, to treat HNSCC. However, this PD-L1/CTLA-4 dual blockade combination did not show better efficacy in HNSCC [72]. CHECKMATE 651 is a Phase III trial using nivolumab combined with ipilimumab in HNSCC patients; however, the preliminary results of this study showed no improvement in survival [73]. Other studies using oncolytic virus [74], HPV vaccine [75], or histone deacetylase (HDAC) inhibitor [76] in combination with anti-PD-1

treatment have shown modest improvements in ORR for HNSCC. The results of these studies demonstrate the potential of various anti-PD-1 combination therapies for the treatment of HNSCC patients. With proper biomarker research, a multi-dimensional and personalized approach may be developed to guide the use of combination strategies in HNSCC patients.



- **Next steps: extend the DoR achieved for afatinib plus pembrolizumab combination therapy**

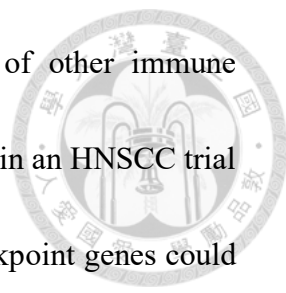
This study showed improved ORR among HNSCC patients using afatinib combined with pembrolizumab. However, the extent to which afatinib contributes to improved pembrolizumab efficacy remains unclear. In addition, the DoR recorded for this study was shorter than the DoR reported for either pembrolizumab or nivolumab monotherapy [17, 18, 41]. To clarify the contribution of afatinib and examine the reasons for the shorter DoR, we referenced the results of a pembrolizumab neoadjuvant trial performed by Uppaluri et al., which enrolled 36 HNSCC patients [77]. In this study, eligible patients received one dose of pembrolizumab monotherapy, followed by curative surgery 2–3 weeks after administration of neoadjuvant therapy. Gene set enrichment analysis of paired, pre- and post- treatment tissue samples (n = 15) showed that pembrolizumab monotherapy induced the upregulation of the following gene sets:



IFN- α response, IFN- γ response, inflammatory response, allograft rejection, tumor necrosis factor-alpha signaling via nuclear factor kappa B, and interleukin-6–JAK–STAT3 signaling. In the present study, afatinib–pembrolizumab combination therapy upregulated gene sets related to antigen presentation. However, the gene sets related to the IFN- γ response and IFN- α response were not elevated. The IFN- γ signature has been identified as a biomarker for predicting successful pembrolizumab monotherapy in several cancer types, including HNSCC [78]. The shorter DoR observed for afatinib–pembrolizumab combination therapy may be due to the insufficient induction of the IFN response. Although cross-trial comparisons should be interpreted with caution, we postulate that afatinib may partially improve pembrolizumab efficacy by augmenting antigen presentation. However, an insufficient induction of an IFN reaction may explain the shorter DoR of the afatinib–pembrolizumab combination.

- **Mechanisms of acquired resistance to afatinib plus pembrolizumab combination therapy: what do we know?**

Anti–PD-1 therapy alone can induce tumor resistance against treatment; however, combined therapy might also induce resistance. Our gene analysis data from post-progression tissues indicated the potential for acquired resistance in response to this combination therapy. The upregulation of LAG3, an immune checkpoint gene, was

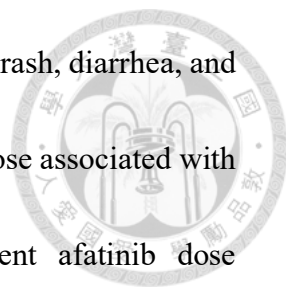


identified in some post-treatment specimens. The upregulation of other immune checkpoint genes in the tumor microenvironment has been reported in an HNSCC trial using neoadjuvant pembrolizumab [77]. Upregulated immune checkpoint genes could represent potential treatment targets in patients with progressive disease following first-line anti-PD-1 therapy. In addition to changes in immune cells, the emergence of new mutations in tumor cells can also modulate immune regulation [33]. In the post-progression biopsy samples, further gene alterations associated with immune reactivity were identified (*JAK1*, *JAK3*, and *INPP4B*). These gene alterations may contribute to disease progression. In addition, T cell regulation and inhibition may contribute to the development of resistance. In the enrichment analysis, three gene sets related to negative leukocyte and lymphocyte regulatory functions had positive enrichment scores. In all three gene sets, *FOXP3* was identified at the leading edge, implying that regulatory T cells may play an inhibitory role in response to combination therapy. The underlying mechanism requires further investigation. Tu et al. [79] showed that afatinib might suppress T cell function in the peripheral immune cells of lung cancer patients and decrease the effects of immune therapy. Our study and Tu's study both demonstrated the possibility that anti-PD-1 combination treatments could simultaneously enhance immune reactivity through some mechanisms while suppressing immune function through other mechanisms. Fine-tuning the balance

between immune activation and suppression may represent a key component for extending the survival of patients undergoing anti-PD-1 combination therapy. In conclusion, the increased expression of other immune checkpoints, immunosuppressive pathways, and the emergence of new gene alterations involved in immune reactivity may contribute to acquired resistance in anti-PD-1-based combination therapy approaches.

- **Toxicities associated with afatinib plus pembrolizumab therapy in HNSCC**

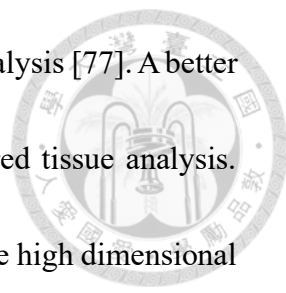
The potential toxicity of anti-PD-1 and EGFR-TKI combination therapies, especially the incidence of pneumonitis, had been described in several lung cancer studies [80, 81], which have described a high incidence of treatment-related pneumonitis. In our study, one patient (1/29, 3.4%) experienced a Grade 2 treatment-related pneumonitis event. Differences in the incidence of pneumonitis between these anti-PD-1/PD-L1-EGFR-TKI studies may be due to differences in the cancer types of patients. A meta-analysis showed that lung cancer patients experience a higher incidence of pneumonitis during anti-PD-1/PD-L1 therapy, whereas the incidence of pneumonitis occurred at similar rates among other cancer types during anti-PD-1/PD-L1 therapy [82], which may account for the increased incidence of pneumonitis reported in studies using anti-PD-1/PD-L1 combined with EGFR-TKIs to treat NSCLC



patients. In the present study, the most common toxicities were skin rash, diarrhea, and paronychia, and the patterns of skin rash reporter were similar to those associated with EGFR-TKI treatment. In addition, 41.2% of patients underwent afatinib dose reductions due to treatment-related toxicity. An ongoing Phase II trial is examining the use of afatinib at 30 mg daily combined with anti-PD-1 for esophageal cancer patients in Taiwan (BEAR study, NCT04839471), which might contribute to determining the optimal afatinib dosage in combination with anti-PD-1 therapy.

- **Limitations of this prospective study**

Comparing pre- and post-treatment biopsy results can provide useful information regarding the efficacies and biological effects of study treatment in the tumor. In the present study, we examined 9 (31%) pairs of pre- and post-treatment biopsy specimens for study. Not all patients had paired biopsies for a variety of reasons, including the patient's reluctance to undergo a second biopsy, disease progression, biopsy risks (i.e., too close to major vessels), and tumors that became too small to obtain biopsies. Several strategies could be applied to future studies to improve the successful acquisition of paired biopsy for analyses. A neoadjuvant study followed by surgical tumor resection may provide a better window of opportunity for obtaining pre- and post-treatment samples. For example, a neoadjuvant pembrolizumab trial for HNSCC patients



acquired paired tissue samples from 42% (15/36) of the cohort for analysis [77]. A better analysis technique that requires less tissue may also facilitate paired tissue analysis. Single-cell technologies [83] and spatial proteomics [84] can provide high dimensional information using less tissue. Liquid biopsies [85] are a less invasive approach for monitoring change in tumors and may represent a feasible approach for recurrent or metastatic tumor sites that are not easy to biopsy. For patients whose tumors shrink quicker than expected, an earlier biopsy timing may increase the acquisition rate of re-biopsy. For patients who are reluctant for biopsy or experience disease progression, a better patient support may increase the willingness of re-biopsy.

This study was associated with other several limitations. The small sample size may overestimate the efficacy of the treatment regimen. In this study, we used bulk RNA from the entire tumor biopsy sample to perform analyses, which did not allow for differential gene expression comparisons between tumor and immune cells or between different immune cell subsets. Approximately 44% of our enrolled patients had previously experienced two or more lines of palliative therapy, and 35% of enrolled patients were primarily resistant to concurrent chemoradiation within six months. These patients typically present with worse prognoses and may have worse survival than platinum-naïve or platinum-sensitive HNSCC patients, which might have contributed to the lack of significantly prolonged OS in this study. The efficacy of afatinib–

pembrolizumab combination therapy for the treatment-naïve or platinum-sensitive patients is worthy of further exploration.



- **A journey in CyTOF study: lessons learned**

We explored the possibility of using CyTOF for studying the heterogeneity of immune cells in the tumor microenvironment. We identified potential heterogeneity among immune cells according to chemokine receptor expression patterns. Several clusters of CD8⁺ and CD4⁺ T cells were identified in the analysis. In our analysis in **Figure 6**, we also found that CXCL13 and CXCL9 were elevated after taking combination therapy. Further exploration using CyTOF and bulk mRNA analysis in tumors may help us to know the interaction of chemokines and chemokine receptors in tumor microenvironment. The emergence of new single-cell mRNA analysis methods has improved data quality and expanded the dimensions of available data. New multi-omics spatial analyses also allow for multi-omics analyses to be conducted using commonly acquired pathological specimens. By utilizing these tools, we can disclose the interaction of tumor cells and immune cells in the microenvironment.

- **Conclusion**

In conclusion, this study demonstrated the efficacy of afatinib plus pembrolizumab combination therapy for patients with HNSCC. By utilizing a multi-omics approach and bioinformatics analyses, the study showed that enhancing the antigen presentation machinery may be a key event in improving therapeutic efficacy for the combination of afatinib plus pembrolizumab. The genomics analysis revealed that unaltered MTAP might serve as a potential biomarker able to predict the clinical response to treatment. By using open cancer data analysis, the study found that tumors with unaltered MTAP present a favorable tumor microenvironment amenable to anti-PD-1 therapy. The CyTOF approach showed the feasibility of single-cell proteomics analysis. Further applications and explorations could be considered.



Chapter 6 Future works



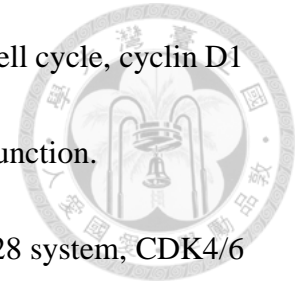
6.1 Real-world analysis of anti-PD-1 therapy in patients with HNSCC and accompanying biomarker analysis

Anti-PD-1 therapy has been used for the treatment of HNSCC for many years, and a substantial number of patients have been treated with anti-PD-1 therapies. We found that a small group of patients presented with a durable response after receiving a short course of anti-PD-1 therapy, which was maintained using afatinib. We plan to analyze the characteristics of these patients and their tumor microenvironments.

6.2 Ribociclib, an anti-CDK4/6 inhibitor, combined with anti-PD-1 for HNSCC treatment

Cell cycle alterations are common mutations associated with HNSCC. In an analysis of the HNSCC TCGA dataset [86], 96% of HPV-unrelated HNSCC tumors presented with cell cycle dysregulation. In the TCGA analysis [86], 58% of HPV-unrelated HNSCC tumors had mutations or homozygous deletions detected in *CDKN2A*, which encodes cyclin-dependent kinase inhibitor 2A and regulates the cell cycle by inhibiting CDK4 and CDK6. Approximately 31% of HPV-unrelated HNSCC tumors

had *CCND1* amplifications, which encodes cyclin D1 [86]. In the cell cycle, cyclin D1 forms a complex with CDK4 and CDK6 to regulate the cell cycle function.

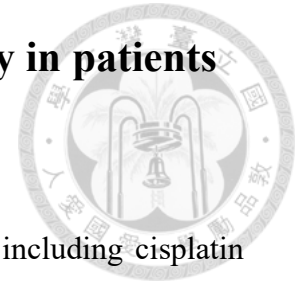


In a drug screening study using Jurkat cells and an anti-CD3/28 system, CDK4/6 inhibitors were identified as a potential mechanism for increasing T cell functions in the tumor microenvironment [87]. In animal studies, CDK4/6 inhibitors decrease tumor growth by suppressing the cell cycle. In addition, CDK4/6 inhibitors induce the expression of HLA and increase antigen presentation. CDK4/6 inhibitors also induce T cell functions and increase T cell infiltration into the tumor [88].

T cell exclusion is a mechanism related to resistance to immunotherapy. CDK4/6 inhibitors can reverse this resistance program in the tumor microenvironment, increasing the immune response in the tumor [89].

Therefore, we initiated a study using ribociclib, a CDK 4/6 inhibitor, combined with spartalizumab, an anti-PD-1 antibody, to treat HPV-unrelated HNSCC. This Phase II study used an expansion cohort to test the toxicity and efficacy of this combination therapy. Biomarkers were analyzed using NGS and mRNA analysis to explore potential biomarkers of response to treatment.

6.3 Personalized anti–PD-1 combination therapy in patients with HNSCC



Currently, anti–PD-1 therapy combined with chemotherapy, including cisplatin and fluorouracil, represents the standard first-line treatment for patients with HNSCC. Many ongoing clinical trials are examining the use of anti–PD-1 therapy combined with different agents to treat HNSCC. These anti–PD-1 combination therapies have shown a modest response rate in patients with HNSCC. In most cases, these studies have not selected proper combinations specific to each patient based on the status of the tumor microenvironment and the genetic background of the tumor. We hypothesize that personalized anti–PD-1 therapies may be possible for patients with HNSCC being treated with anti–PD-1 therapies.

In the first study (ALPHA study), we found that MTAP alterations may predict a poor response rate and poor survival in patients with HNSCC. The second study (RISE-HN) will use a similar strategy to explore possible predictive biomarkers of response to treatment. After the primary analysis of these two trials, these trial data will be merged for further analysis. A retrospective cohort will also be analyzed using a NanoString mRNA panel. We hypothesize that a personalized approach can be achieved by analyzing the status of the tumor microenvironment and the genetic background of the tumor.

Chapter 7 Tables



Table 1 Patient characteristics

	Afatinib + pembrolizumab N = 29
Age (years) Median (range)	53.4 (26.2–71.1)
Sex, n (%)	
Male	27 (93.1)
Female	2 (6.9)
ECOG PS	
0	2 (6.9)
1	27 (93.1)
Habits	
Alcohol	20 (69.0)
Betel nuts	19 (65.5)
Cigarette	23 (79.3)
Primary tumor site, n (%)	
Oral cavity	19 (65.5)
Oropharynx	6 (20.7)
P16+	4 (13.8)
P16–	1 (3.4)
NA	1 (3.4)
Hypopharynx	2 (6.9)
Larynx	2 (6.9)
Disease status at enrollment, n (%)	
Local recurrence only	15 (51.7)
Local recurrence and metastases	11 (37.9)
Metastases only	3 (10.3)
Metastatic sites	
Lung	11 (37.9)
Liver	5 (17.2)
Bone	4 (13.8)
Kidney	2 (6.9)
Types of prior therapy	

Surgical tumor resection	24 (82.8)
Radiotherapy	26 (89.7)
Cetuximab	16 (55.2)
Prior lines of therapy in recurrent/metastatic setting, n (%) *	
None †	10 (34.5)
1	6 (20.7)
2	6 (20.7)
≥3	7 (24.1)
PD-L1 TPS, n (%)	
<1	8 (27.6)
1–49	13 (44.8)
≥50	7 (24.1)
NA	1 (3.4)
PD-L1 CPS, n (%)	
<1	3 (10.3)
1–19	17 (58.6)
≥20	8 (27.6)
NA	1 (3.4)
Tumor mutational burden (TMB)	
Tested, with results, n (%)	25 (86.2)
TMB (mutations/megabase)	
Median (range)	4 (1–8)
1–5, n (%)	19 (65.5)
6–10, n (%)	6 (20.7)
>10, n (%)	0 (0)
NA, n (%)	4 (13.8)

NA: not available; ECOG PS: Eastern Cooperative Oncology Group performance status; PD-L1: programmed death-ligand 1; TPS: tumor proportion score; CPS: combined positive score.

* Only therapies for recurrent/metastatic diseases were counted in this column. Prior induction or adjuvant therapies were not counted in this column.

† Patients with new recurrent/metastatic diseases in 6 months after the last dose of platinum-based therapy in adjuvant therapy or concurrent chemoradiation.

Table 2 Treatment related adverse events

AE, treatment related	Gr. 1	Gr. 2	Gr.3	Gr. 4	Gr. 5
Skin rash	17 (59%)	0 (0%)	4 (14%)	0 (0%)	0 (0%)
Diarrhea	8 (28%)	7 (24%)	4 (14%)	0 (0%)	0 (0%)
Paronychia	8 (28%)	4 (18%)	0 (0%)	0 (0%)	0 (0%)
Mucositis	8 (28%)	3 (10%)	1 (3%)	0 (0%)	0 (0%)
Weight loss	5 (17%)	5 (17%)	0 (0%)	0 (0%)	0 (0%)
Fatigue	6 (21%)	2 (7%)	1 (3%)	0 (0%)	0 (0%)
Anemia	4 (14%)	2 (7%)	1 (3%)	0 (0%)	0 (0%)
Anorexia	5 (17%)	1 (3%)	0 (0%)	0 (0%)	0 (0%)
Creatinine increase	3 (10%)	1 (3%)	1 (3%)	0 (0%)	0 (0%)
Nausea	2 (7%)	3 (10%)	0 (0%)	0 (0%)	0 (0%)
Vomiting	1 (3%)	3 (10%)	0 (0%)	0 (0%)	0 (0%)
ALT increase	2 (7%)	1 (3%)	0 (0%)	0 (0%)	0 (0%)
AST increase	2 (7%)	0 (0%)	0 (0%)	0 (0%)	0 (0%)
ALP increase	1 (3%)	1 (3%)	0 (0%)	0 (0%)	0 (0%)
GGT increase	0 (0%)	1 (3%)	0 (0%)	0 (0%)	0 (0%)
Hypothyroidism	2 (7%)	0 (0%)	0 (0%)	0 (0%)	0 (0%)
Bleeding	0 (0%)	0 (0%)	1 (3%)	0 (0%)	1 (3%)
Pneumonitis	0 (0%)	1 (3%)	0 (0%)	0 (0%)	0 (0%)

AE: adverse event; Gr.: grade; ALT: alanine aminotransferase; AST: aspartate aminotransferase; ALP: alpha-fetoprotein; GGT: gamma-glutamyltransferase.

Chapter 8 Figures

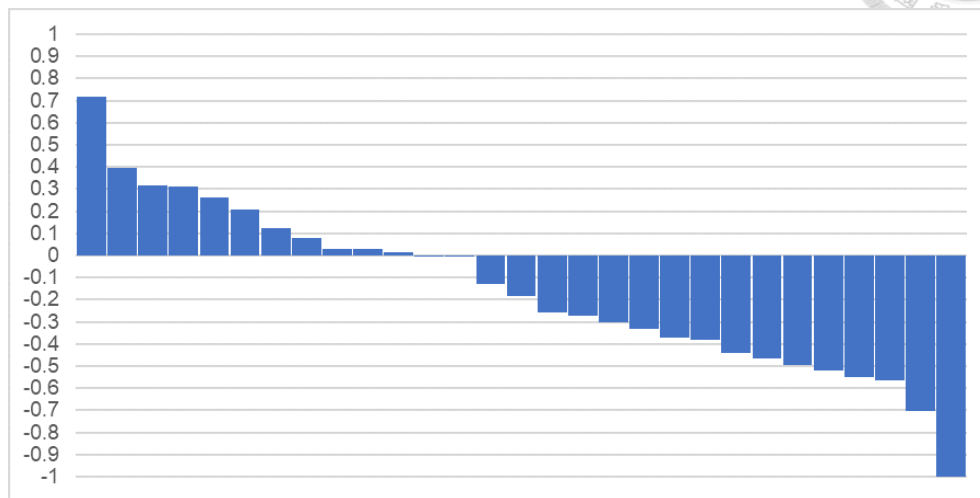


Figure 1 Clinical response rate to afatinib plus pembrolizumab therapy in

HNSCC patients

One patient had a complete response, and 11 patients had a confirmed partial response (overall response rate: 12/29, 41.4% [95% confidence interval (CI): 23.5%–61.1%]).

Stable disease during therapy was registered in 7 of 29 patients (24.1% [95% CI: 10.3%–43.5%]). The overall disease control rate was 65.5% (95% CI: 45.7%–82.1%).

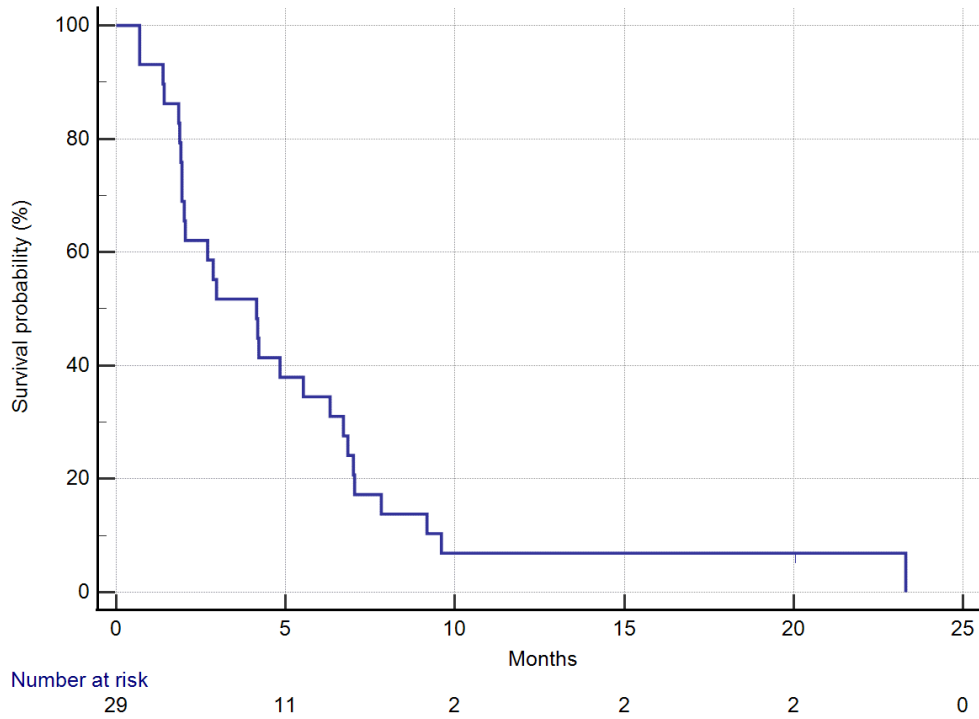


Figure 2 Clinical efficacy of afatinib plus pembrolizumab therapy in HNSCC

patients: progression-free survival

The median progression-free survival was 4.1 months (95% confidence interval: 1.9–6.3 months; n = 29)

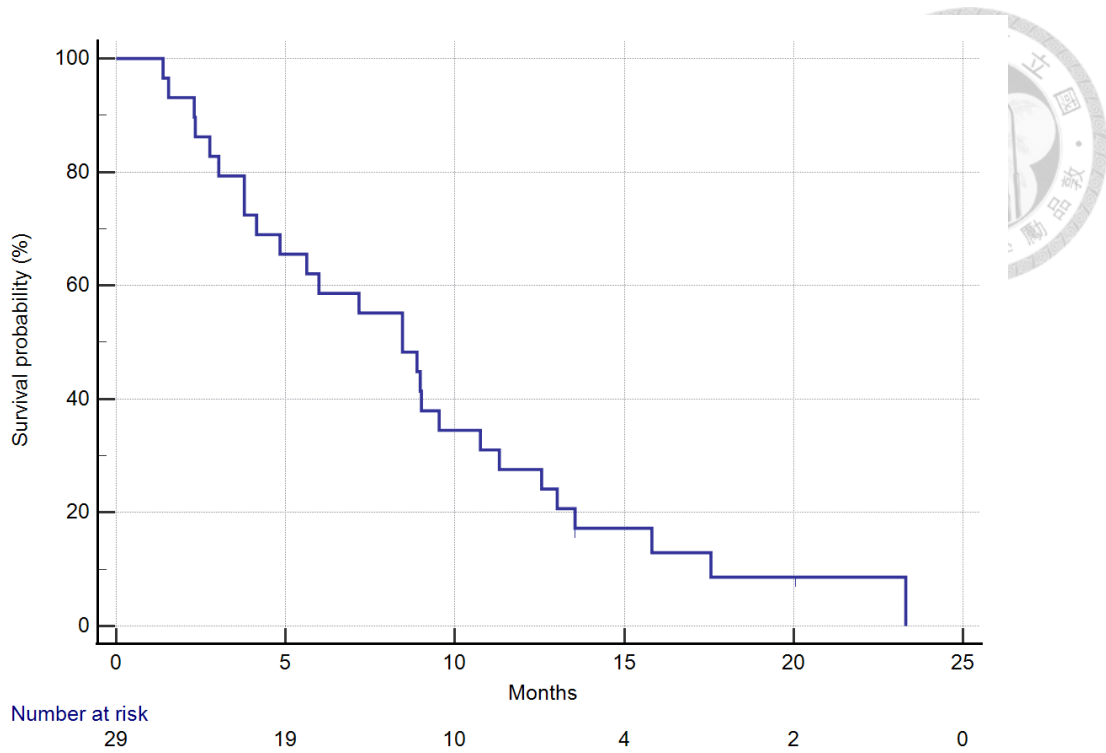


Figure 3 Clinical efficacy of afatinib plus pembrolizumab therapy in HNSCC

patients: overall survival

The median overall survival was 8.4 months (95% confidence interval: 4.1–10.8

months; n = 29)

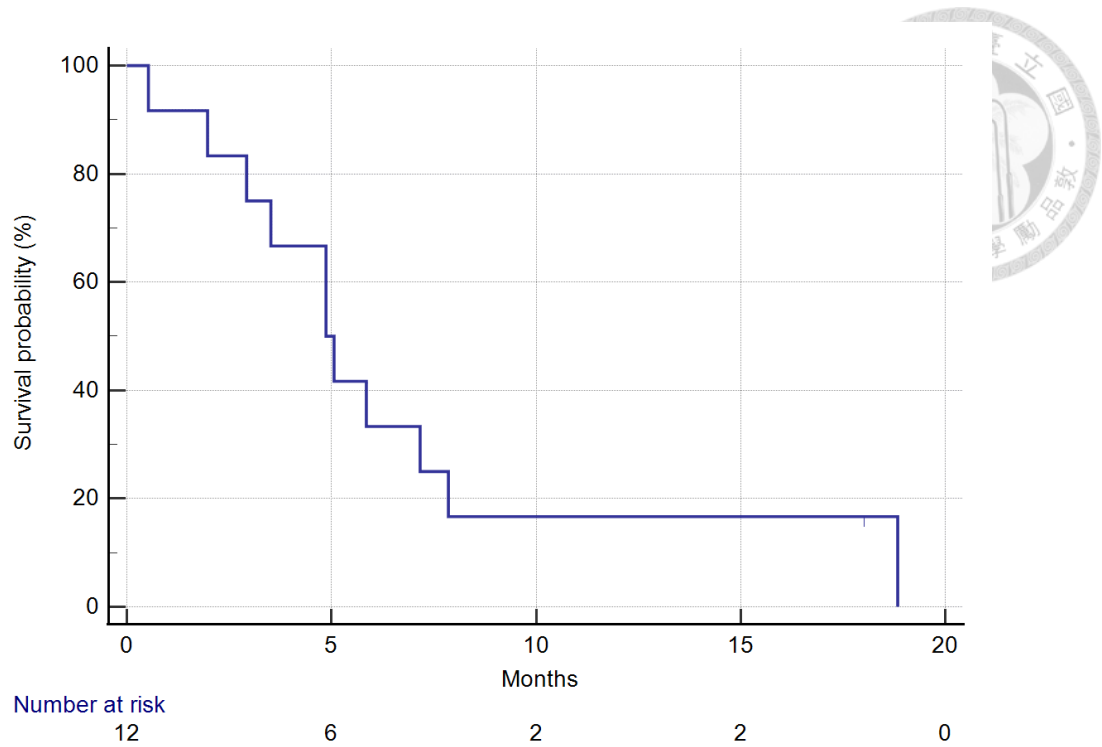


Figure 4 Clinical efficacy of afatinib plus pembrolizumab treatment in HNSCC

patients: the duration of response in responders

The median duration of response was 4.9 months (95% confidence interval: 2.0–7.9 months).

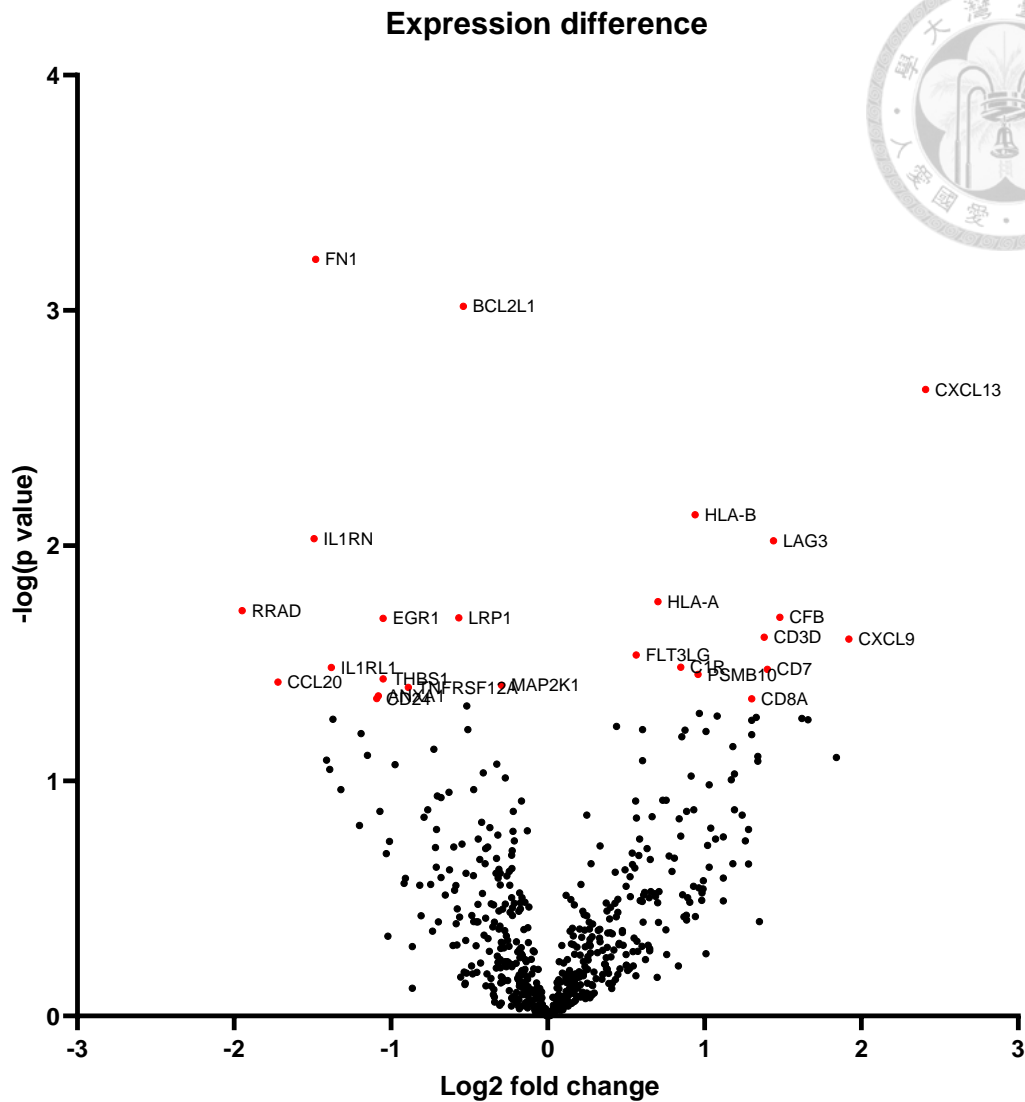


Figure 5 Differential analysis of mRNA expression between paired tissue samples

The mRNA expression levels were compared in nine pairs of tissues (pre-treatment vs. post-treatment). The red dots represent mRNAs with significant differences in pre- vs. post-treatment expression. (Benjamini-Yekutieli method, adjusted $p < 0.05$).

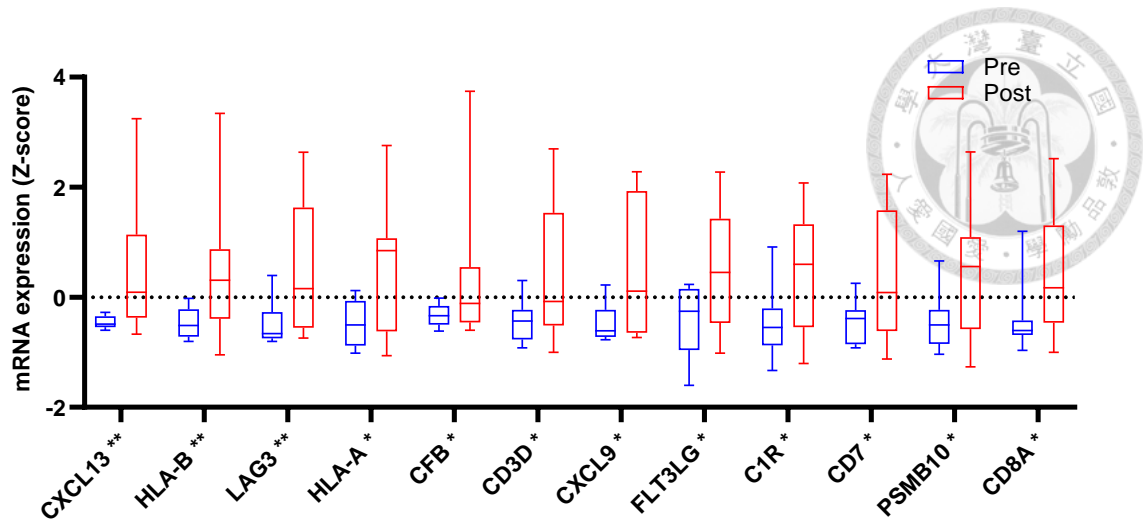


Figure 6 Increased mRNA expression in post-treatment specimens

(Benjamini-Yekutieli method, * $p < 0.05$, ** $p < 0.01$, *** $p < 0.001$)

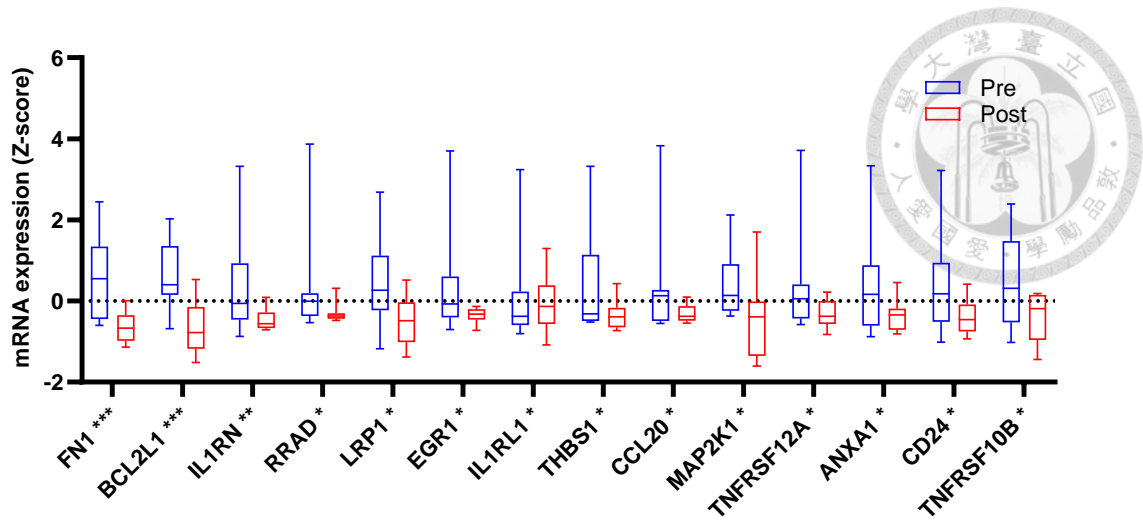


Figure 7 Decreased mRNA expression in post-treatment specimens

(Benjamini-Yekutieli method, * $p < 0.05$, ** $p < 0.01$, *** $p < 0.001$)

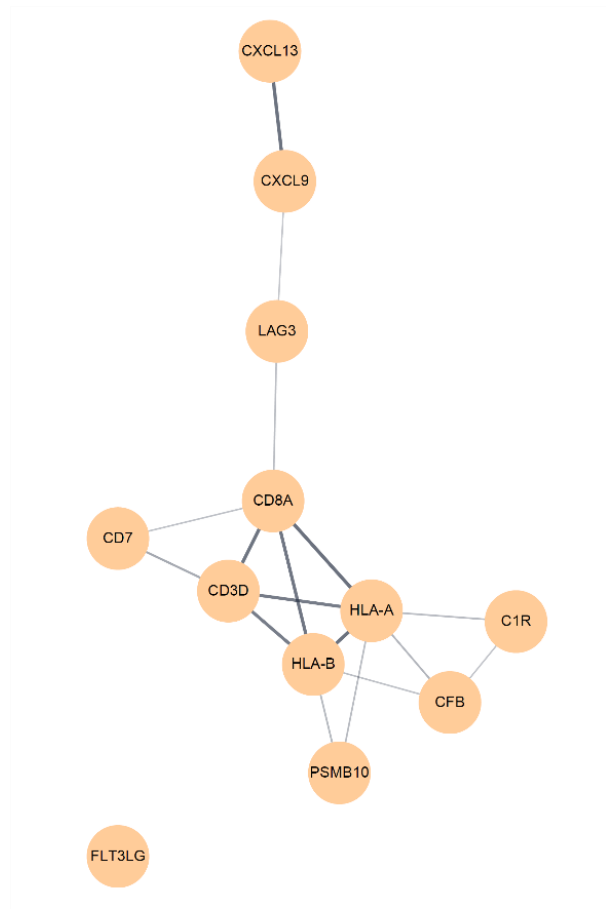


Figure 8 Gene network analysis showing the central role of upregulating antigen presentation machinery in the response to afatinib plus pembrolizumab treatment

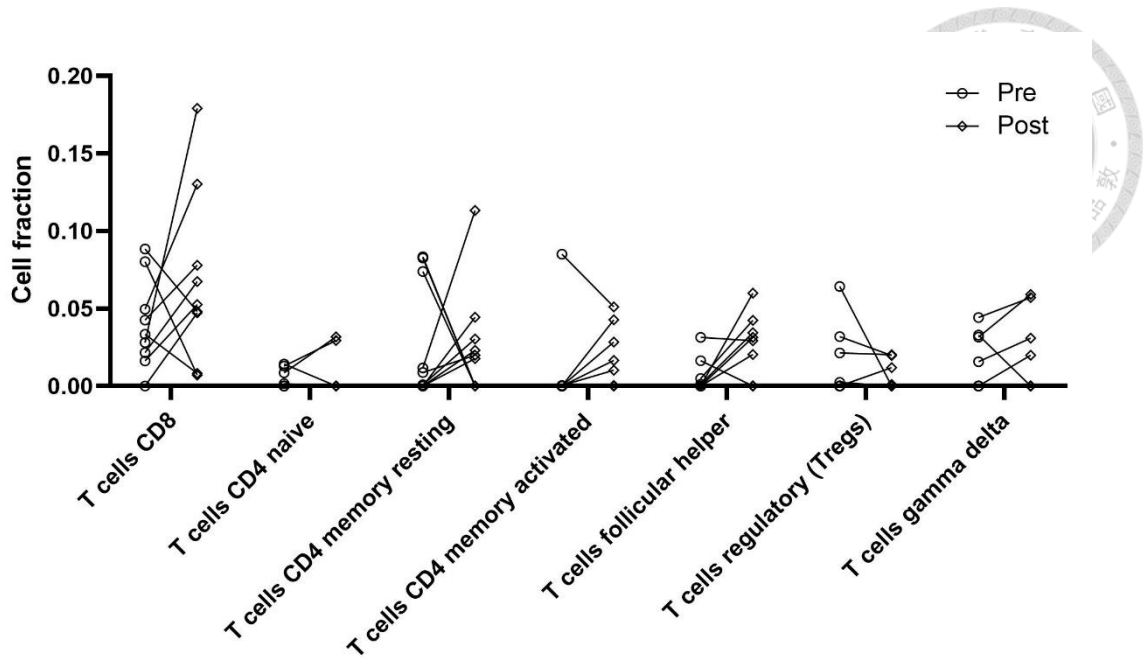


Figure 9 Changes in the T cell fractions within the tumor microenvironment after therapy

In this analysis, using CIBERSORTx and mRNA data, no significant changes in T cell populations were found comparing before and after therapy. However, a trend toward increasing CD8⁺ T cells in the tumor microenvironment was observed.

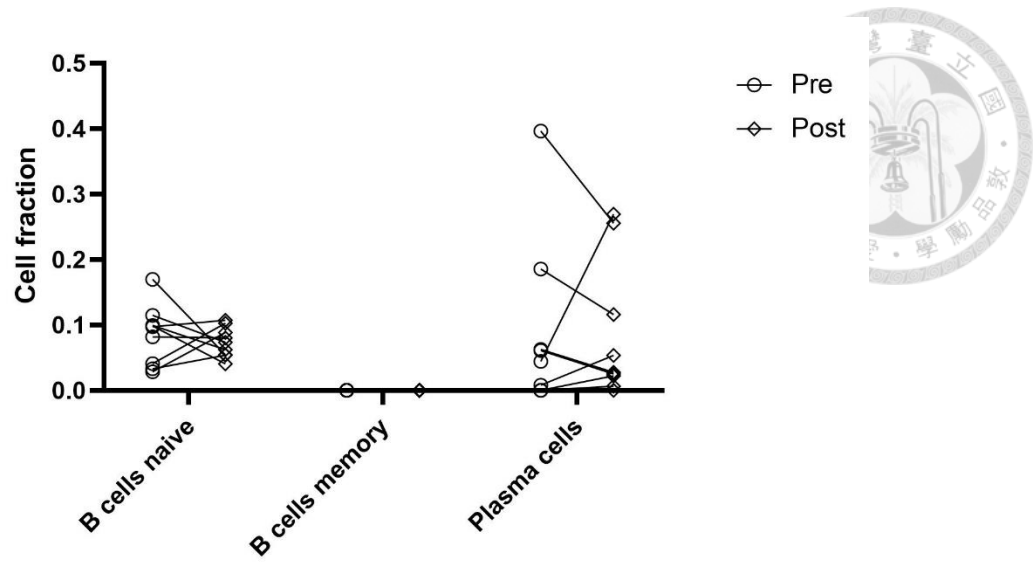


Figure 10 Changes in B and plasma cells in the tumor microenvironment after therapy

No significant changes in B cells were noted in the comparison between before and after therapy.

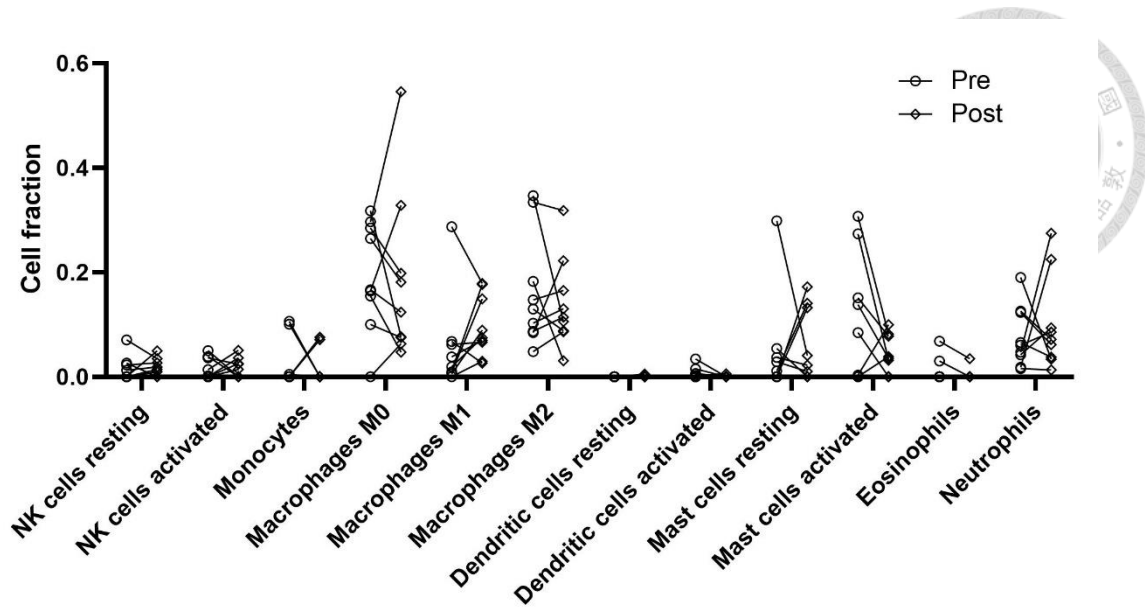


Figure 11 The changes in myeloid cell populations in the tumor

microenvironment after therapy

No significant changes were noted in this study comparing before and after therapy.

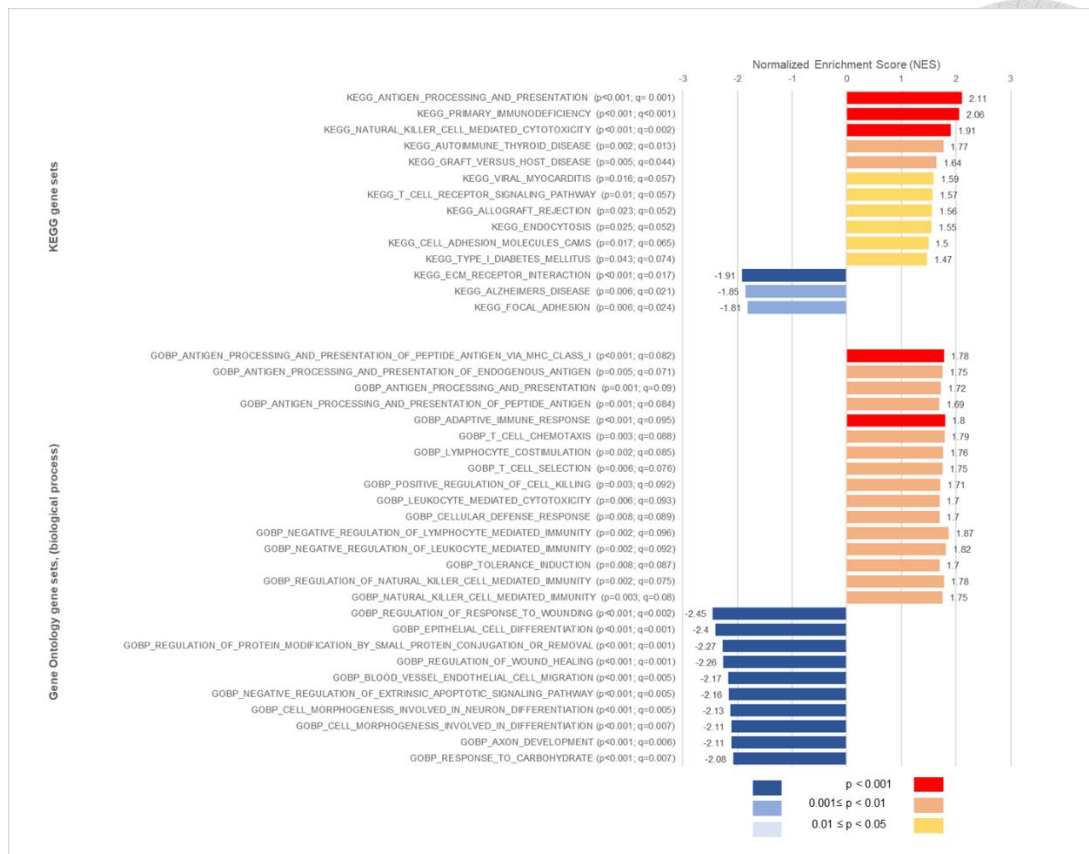


Figure 12 Gene set enrichment analysis of paired tissue mRNA samples

In the enrichment analysis, gene sets related to antigen presentation machinery were upregulated. Gene sets related to tumor growth were down-regulated. (In the GO Biological Process analysis, only the top 10 downregulated gene sets are listed.)



Figure 13 Leading-edge analysis of three gene sets with immune cell regulatory functions.

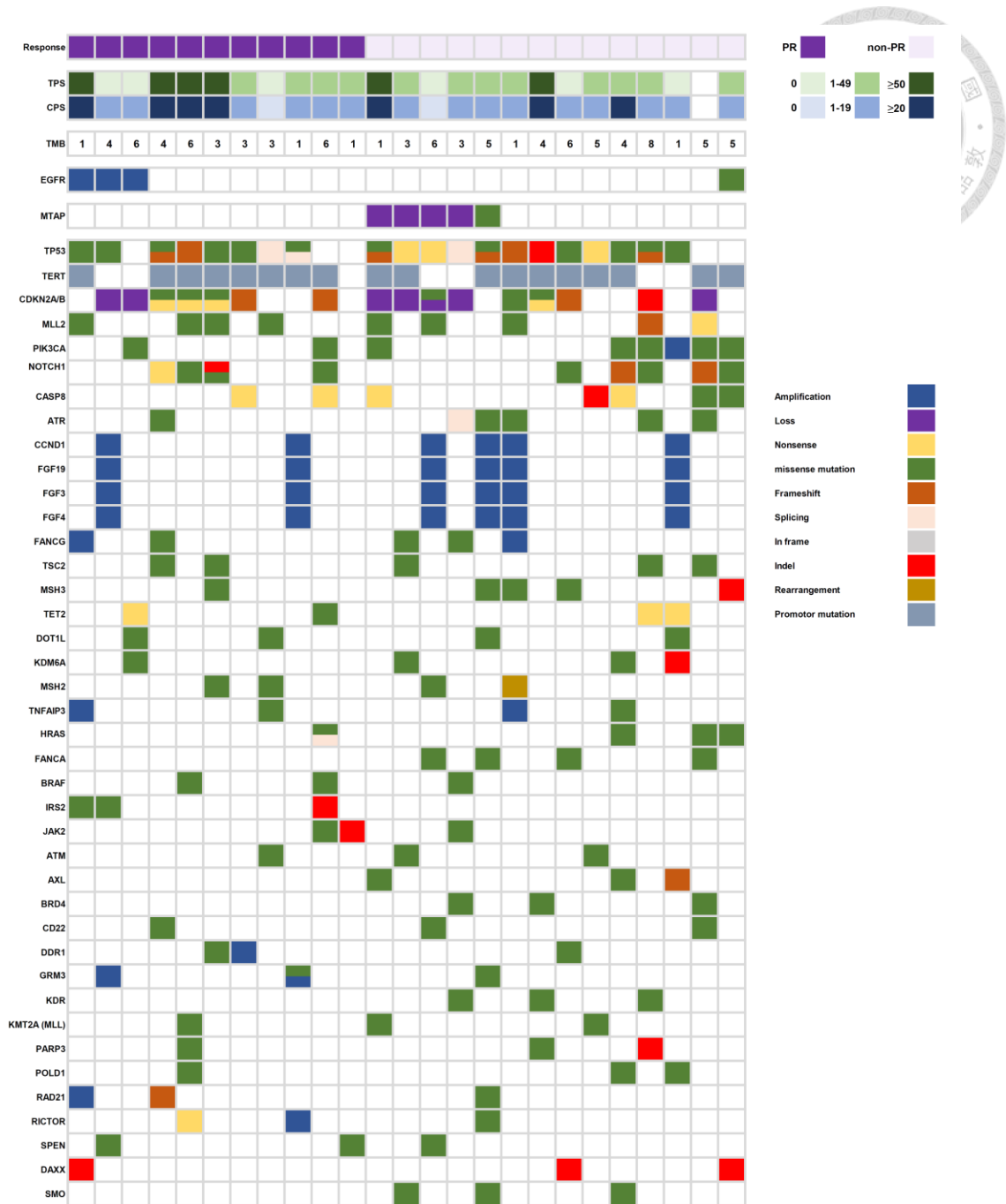


Figure 14 Targeted gene mutation analysis.

Genes were selected if three or more patients had mutations. TMB: tumor mutational burden in mutations/megabase.

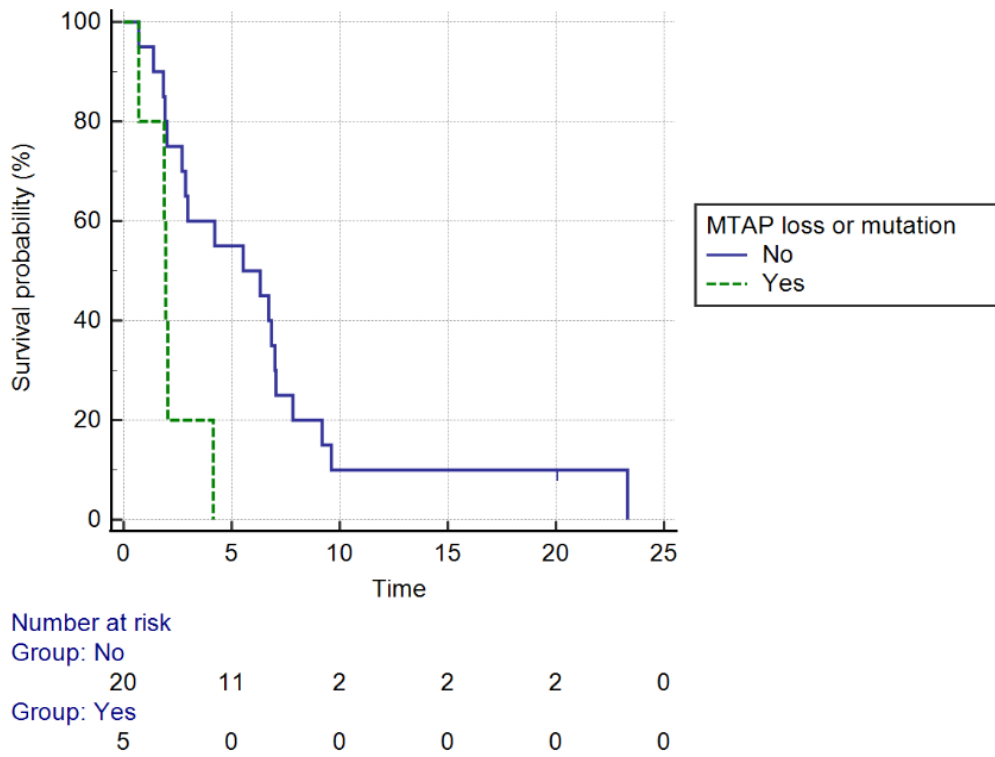


Figure 15 Survival analysis according to *MTAP* status: progression-free survival.

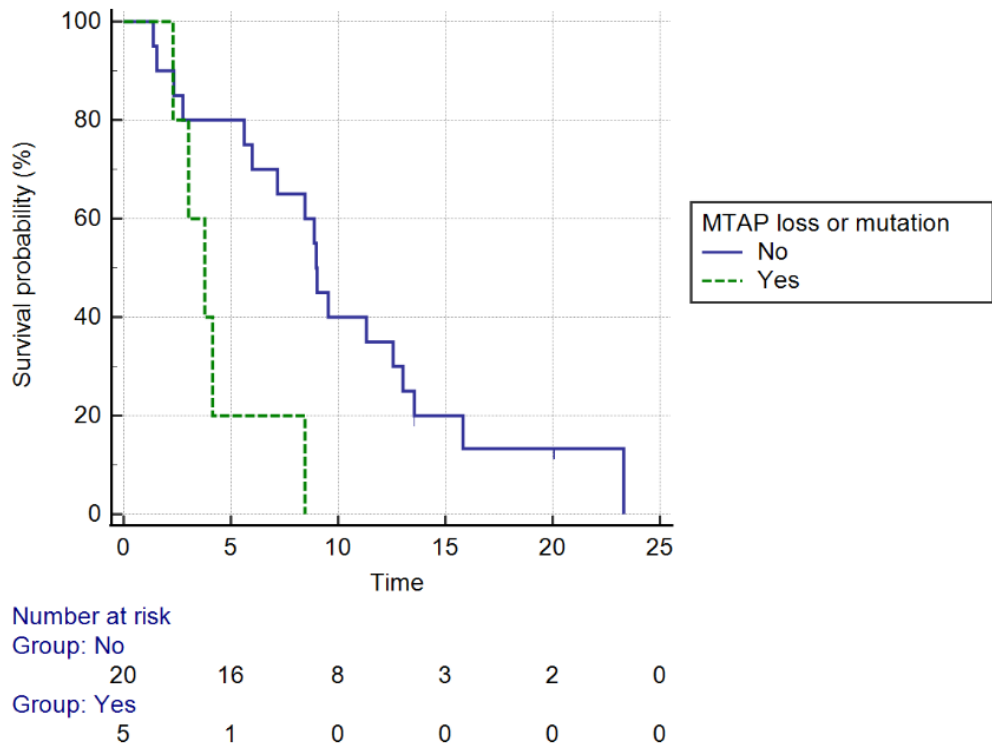


Figure 16 Survival analysis according to *MTAP* status: overall survival

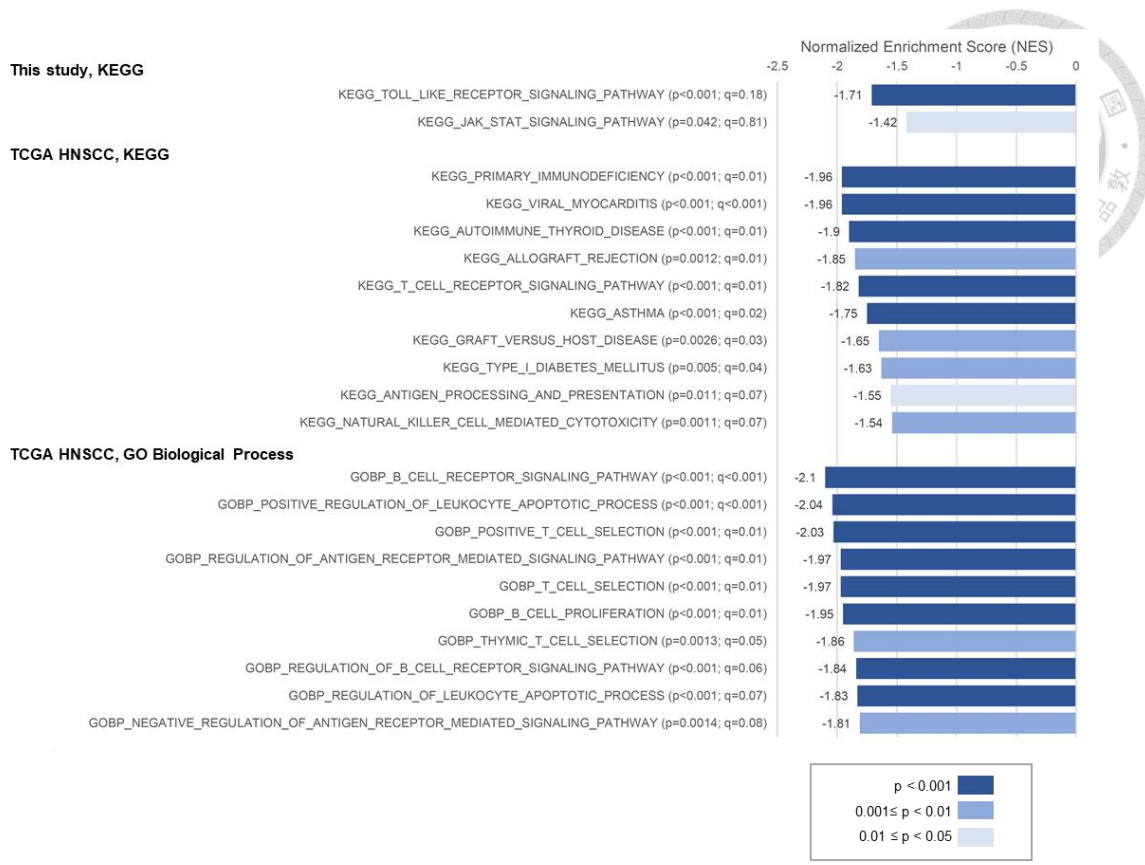


Figure 17 Comparing patients with altered *MTAP* vs. unaltered *MTAP* by gene set enrichment analysis.

In the present study and TCGA HNSCC analyses, tumors with altered *MTAP* had a more suppressed microenvironment.

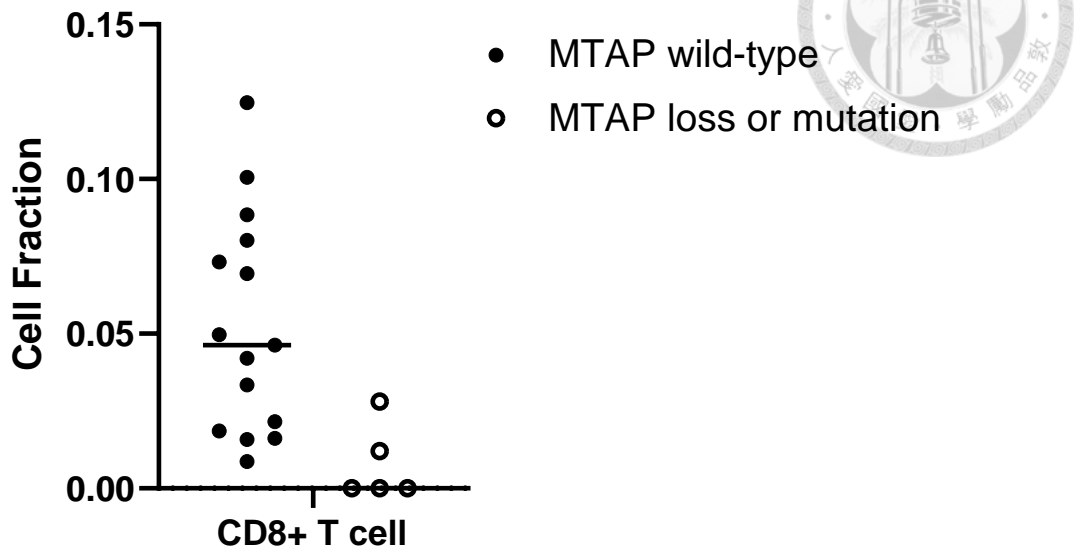


Figure 18 CIBERSORTx analysis comparing altered and unaltered *MTAP* populations

In this study, patients with *MTAP* loss or mutation had a low fraction of CD8⁺ T cells in the tumor microenvironment. (Mann–Whitney U test, $p = 0.0037$, FDR $q = 0.08$)

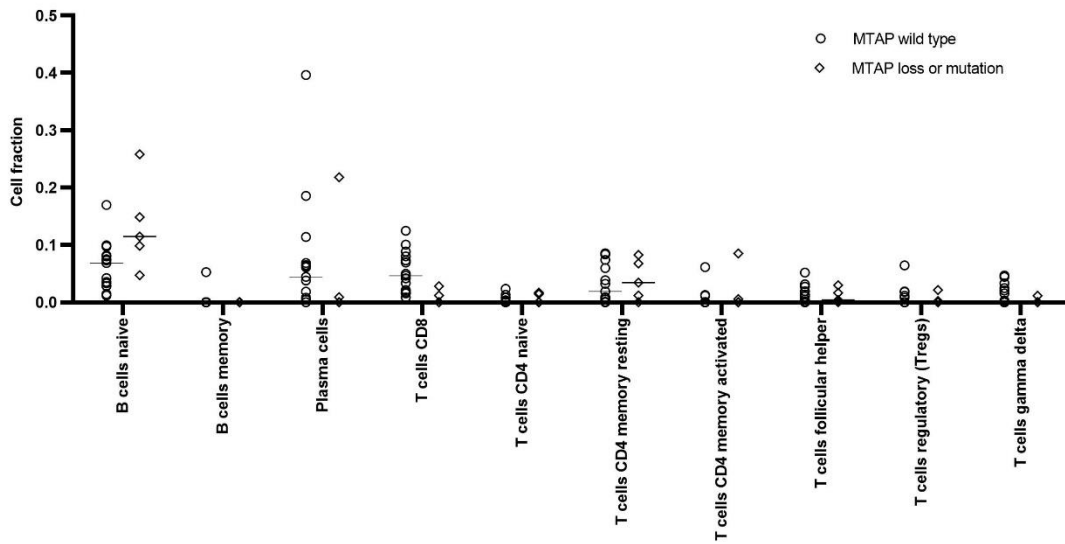


Figure 19 CIBERSORTx analysis comparing the abundance of lymphocytes in patients with altered or unaltered MTAP.

Only CD8+ T cells subsets showed significant differences between unaltered MTAP and altered MTAP subsets.

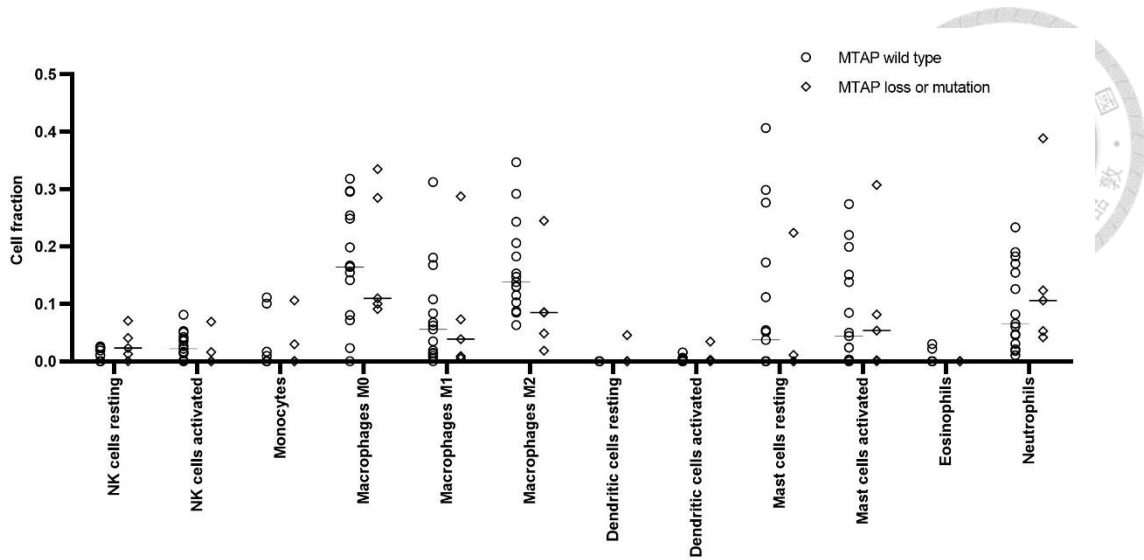


Figure 20 CIBERSORTx analysis comparing the abundance of myeloid cells in patients with altered or unaltered *MTAP*.

No significant differences in myeloid subsets were detected between the two groups.

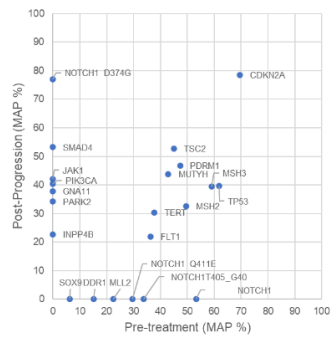
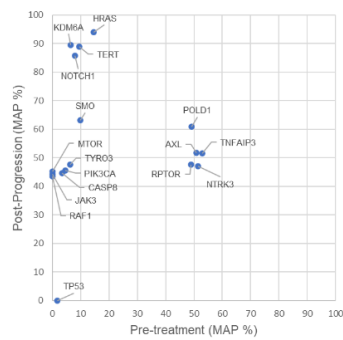
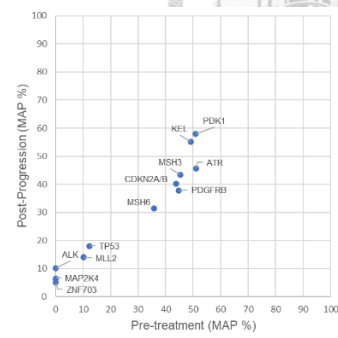
A**B****C**

Figure 21 Differences in mutation allele frequency (MAF) between pre-treatment and post-progression specimens.

A. Best overall response: partial response; B: Best overall response: partial response.

In the post-progression biopsy, a new *MTAP* loss and a new *CDKN2A/B* loss were detected; C: The best overall response of the patient was disease progression.

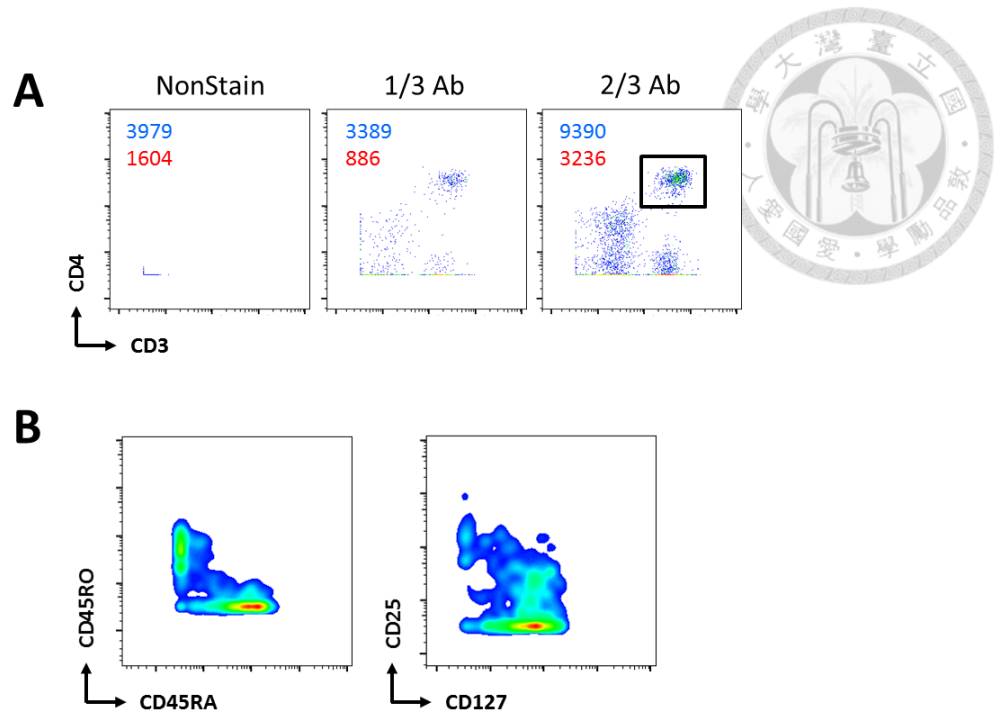


Figure 22 CyTOF pilot experiment

One million peripheral blood mononuclear cells, unstained or stained with 1/3 or 2/3 of recommended antibodies, using the Maxpar staining protocol. (A) The results of different staining conditions. The numbers in blue denote the total events acquired by CyTOF, and the numbers in red denoted DNA⁺ events. (B) The expression pattern of CD45RA versus CD45RO and CD127 versus CD25 in CD4⁺CD3⁺ T cells gated in panel A.

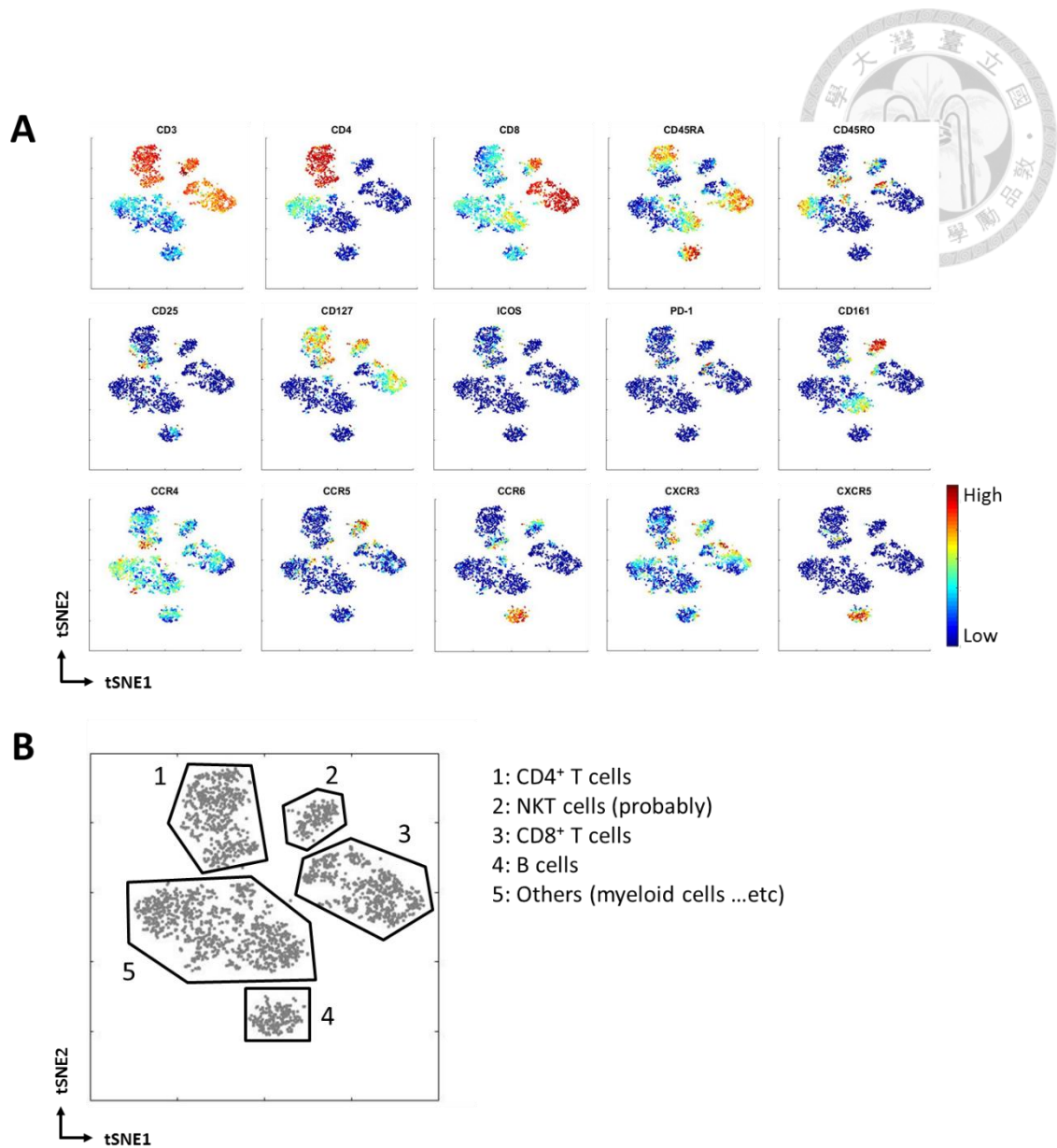


Figure 23 t-SNE analysis of peripheral blood mononuclear cells

Data from the pilot experiment were analyzed. (A) Cells are colored according to the normalized expression of the indicated markers on the t-distributed stochastic neighbor embedding (t-SNE) map. The expression intensity is color-coded, as indicated. (B) Cells were manually grouped and annotated according to the expression patterns identified in panel A.

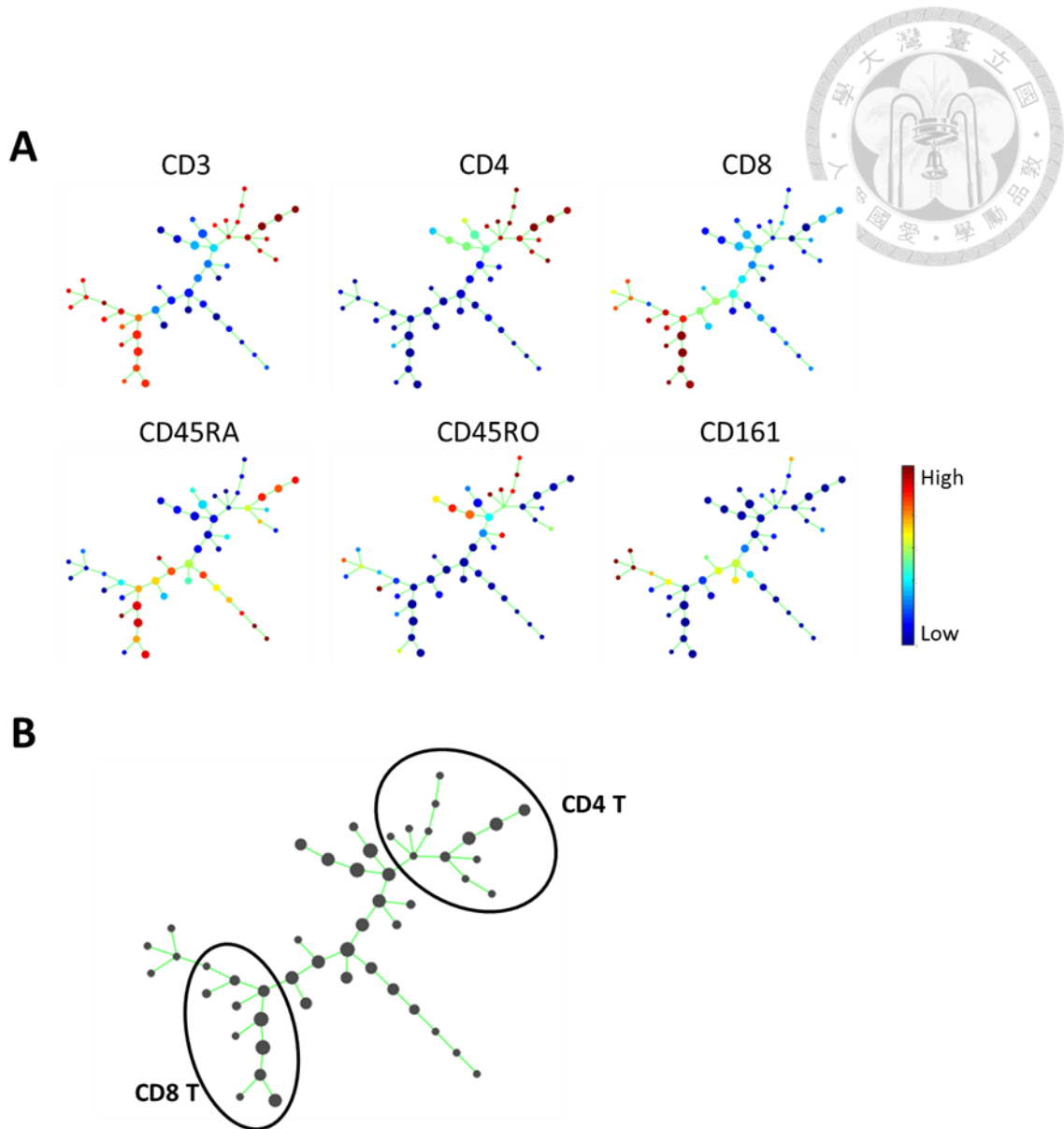


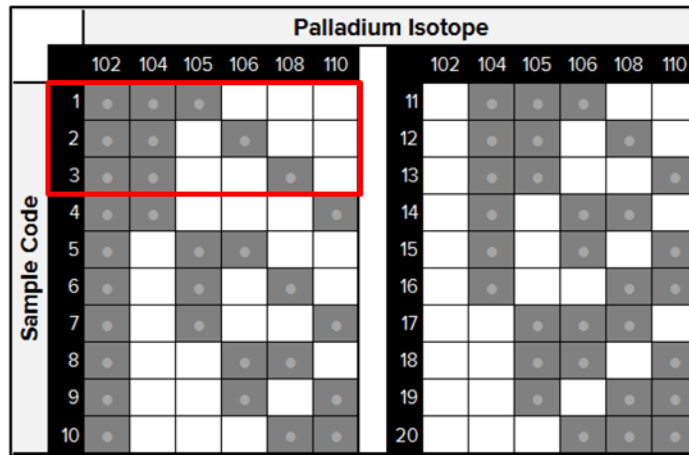
Figure 24 SPADE analysis of peripheral blood mononuclear cells

Data from the pilot experiment were analyzed using spanning-tree progression analysis for density-normalized events (SPADE). (A) Nodes are colored according to the expression levels of the indicated markers on the SPADE tree. The expression intensity is color-coded, as indicated. The circle size indicates the relative cell numbers within the population of each node. (B) Nodes were manually grouped and

annotated according to the expression patterns identified in panel A.



A



B

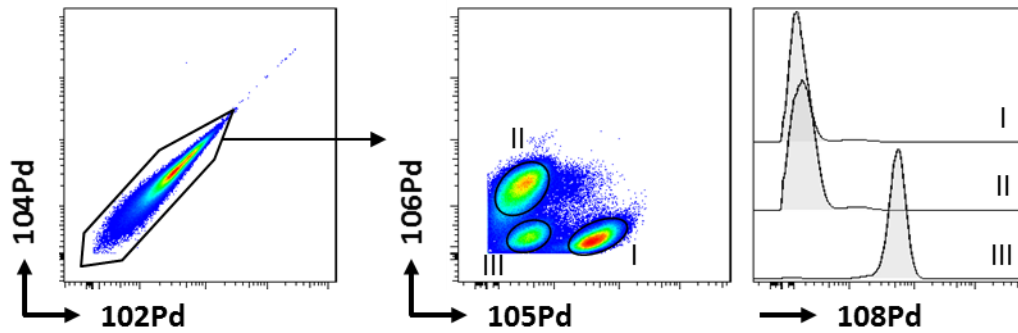


Figure 25 Cell-ID 20-Plex Pd barcoding kit analysis

Peripheral blood mononuclear cells from three individuals were labeled with different barcodes according to the manufacturer's instructions. (A) Sample codes 1, 2, and 3 were used for labeling. (B) Data acquired by CyTOF was analyzed by FlowJo. 108Pd signals were examined among populations I, II, and III.

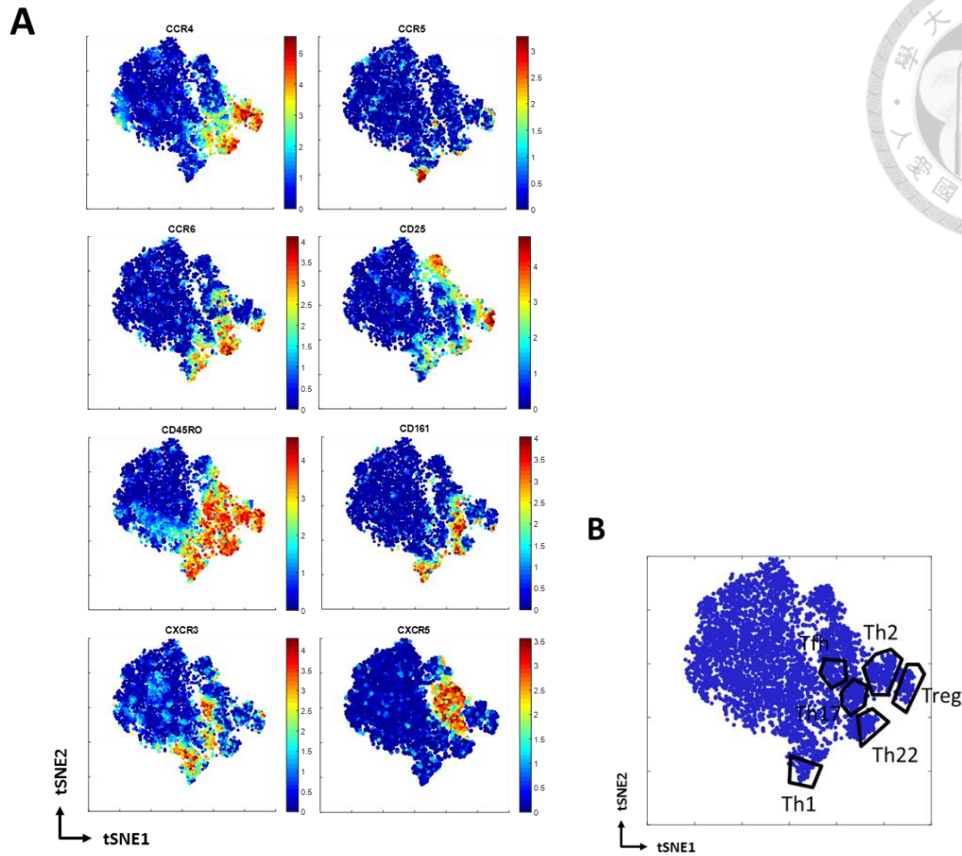



Figure 26 T helper cell location on the t-SNE map of CD4⁺ T cells.

CD4⁺CD3⁺ cells were gated for t-distributed stochastic neighbor embedding (t-SNE) analysis. (A) Cells are colored according to the normalized expression of the indicated markers on the t-SNE map. Expression intensity is shown color-coded, as indicated. (B) Cells were manually grouped and annotated according to the expression patterns identified in panel A.

A

Identity		Chemokine Receptor		Exhaustion
CD3	CD11c	CCR1	CXCR1	PD-1
CD4	CD14	CCR2	CXCR2	PD-L1
CD7	CD68	CCR3	CXCR3	CTLA-4
CD8a	CD123	CCR4	CXCR4	TIM-3
FOXP3	CD45	CCR5	CXCR5	Ki-67
CD127	CD19	CCR6	CXCR6	
CD45RA	HLA-DR	CCR7	CX3CR1	
CD16	CD27	CCR8		
		CCR9		
		CCR10		

B


Cell Type	Marker
CD4+ T cell	CD3+ CD4+
CD8+ T cell	CD3+ CD8+
NK cell	CD3- CD7+
B cell	CD19+
Monocyte	CD14+
Macrophage	CD68+
DC	CD11c+
pDC	CD123+

Figure 27 Panel design for CyTOF analysis

(A) Markers used in the panel design. (B) Cell types identified using the marker panel

shown in panel A.

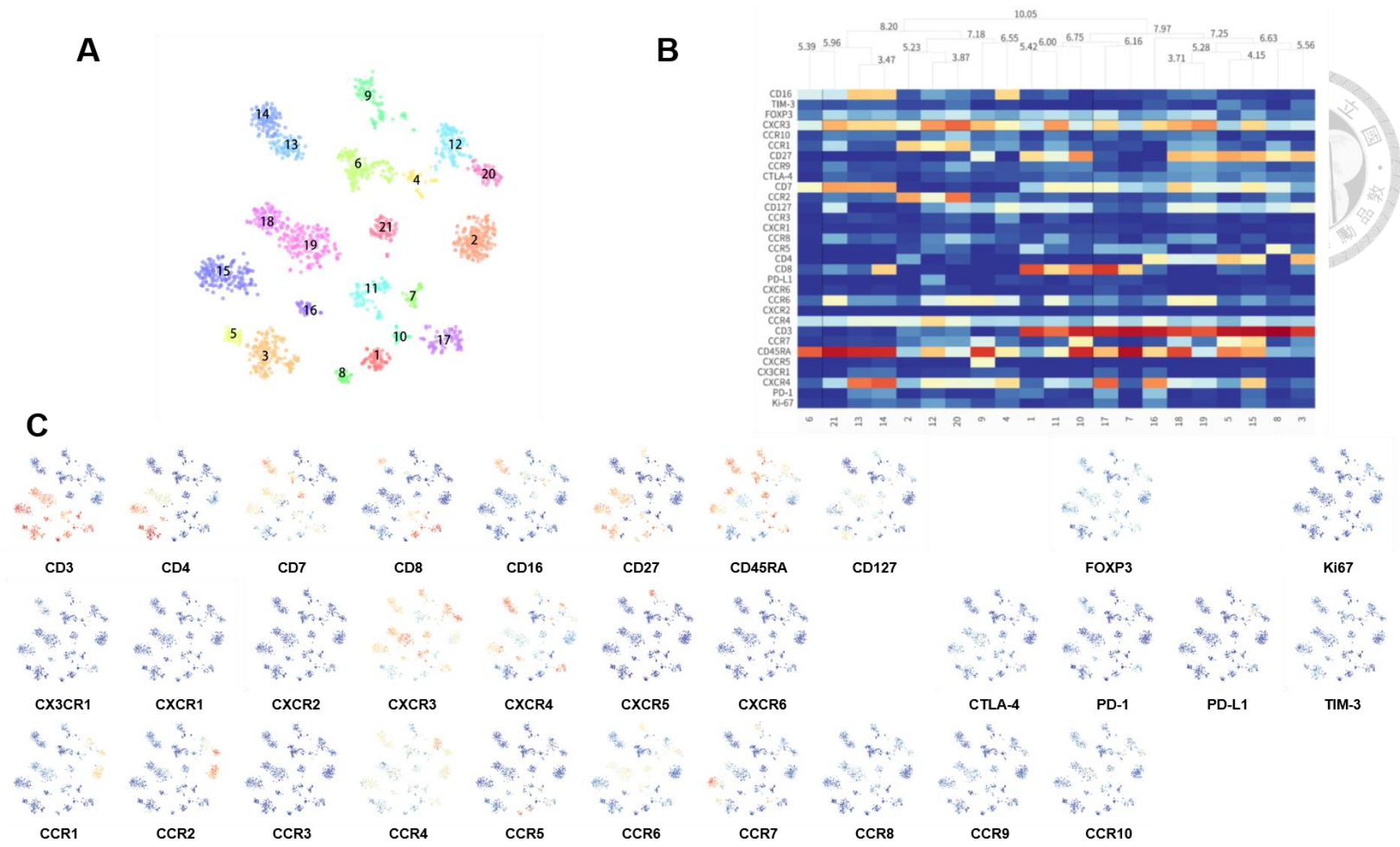


Figure 28 Summary of results for the CyTOF study of peripheral blood mononuclear cells in HNSCC patients

(A) Clustered t-distributed stochastic neighbor embedding (t-SNE) map of peripheral blood mononuclear cells. (B) Heatmap of chemokine receptors and other cell surface markers and checkpoints. (C) The distribution of single-cell markers in the clustered t-SNE map.

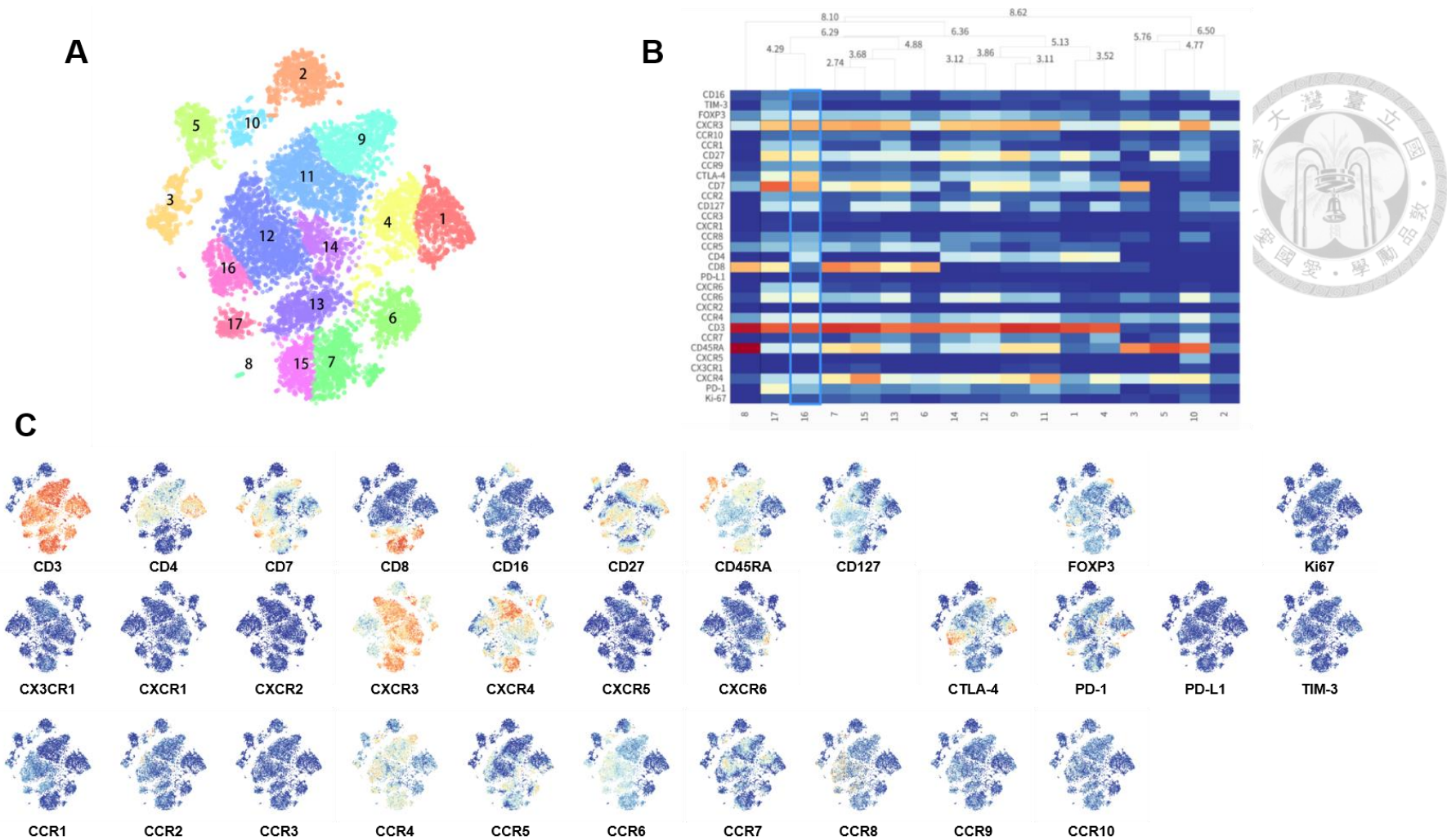


Figure 29 Summary of results for the CyTOF study of tumor-infiltrating lymphocytes in HNSCC patients

(A) Clustered t-distributed stochastic neighbor embedding (t-SNE) map of tumor-infiltrating lymphocytes. (B) Heatmap showing chemokine receptors and other cell surface markers and checkpoints. (C) The distribution of single-cell markers in the clustered t-SNE map.



Chapter 9 Reference

1. Health Promotion Registration MoHaW, Taiwan: **Cancer Registry Annual Report, 2011, Taiwan.** 2014.
2. Hsu WL, Chien YC, Chiang CJ, Yang HI, Lou PJ, Wang CP, Yu KJ, You SL, Wang LY, Chen SY *et al*: **Lifetime risk of distinct upper aerodigestive tract cancers and consumption of alcohol, betel and cigarette.** *Int J Cancer* 2014, **135(6):1480-1486.**
3. Argiris A, Karamouzis MV, Raben D, Ferris RL: **Head and neck cancer.** *The Lancet* 2008, **371(9625):1695-1709.**
4. Cooper JS, Pajak TF, Forastiere AA, Jacobs J, Campbell BH, Saxman SB, Kish JA, Kim HE, Cmelak AJ, Rotman M *et al*: **Postoperative concurrent radiotherapy and chemotherapy for high-risk squamous-cell carcinoma of the head and neck.** *N Engl J Med* 2004, **350(19):1937-1944.**
5. Bernier J, Dommenege C, Ozsahin M, Matuszewska K, Lefebvre JL, Greiner RH, Giralt J, Maingon P, Rolland F, Bolla M *et al*: **Postoperative irradiation with or without concomitant chemotherapy for locally advanced head and neck cancer.** *N Engl J Med* 2004, **350(19):1945-1952.**
6. Bartlett DB, Firth CM, Phillips AC, Moss P, Baylis D, Syddall H, Sayer AA, Cooper C, Lord JM: **The age-related increase in low-grade systemic inflammation (Inflammaging) is not driven by cytomegalovirus infection.** *Aging Cell* 2012, **11(5):912-915.**
7. Posner MR, Hershock DM, Blajman CR, Mickiewicz E, Winkquist E, Gorbounova V, Tjulandin S, Shin DM, Cullen K, Ervin TJ *et al*: **Cisplatin and fluorouracil alone or with docetaxel in head and neck cancer.** *N Engl J Med* 2007, **357(17):1705-1715.**
8. Vermorken JB, Remenar E, van Herpen C, Gorlia T, Mesia R, Degardin M, Stewart JS, Jelic S, Betka J, Preiss JH *et al*: **Cisplatin, fluorouracil, and docetaxel in unresectable head and neck cancer.** *N Engl J Med* 2007, **357(17):1695-1704.**
9. Lorch JH, Goloubeva O, Haddad RI, Cullen K, Sarlis N, Tishler R, Tan M, Fasciano J, Sammartino DE, Posner MR *et al*: **Induction chemotherapy with cisplatin and fluorouracil alone or in combination with docetaxel in locally advanced squamous-cell cancer of the head and neck: long-term results of the TAX 324 randomised phase 3 trial.** *Lancet Oncol* 2011, **12(2):153-159.**
10. Vermorken JB, Mesia R, Rivera F, Remenar E, Kawecki A, Rottey S, Erfan J,

- Zabolotnyy D, Kienzer HR, Cupissol D *et al*: **Platinum-based chemotherapy plus cetuximab in head and neck cancer**. *N Engl J Med* 2008, **359**(11):1116-1127.
11. Chung CH, Ely K, McGavran L, Varella-Garcia M, Parker J, Parker N, Jarrett C, Carter J, Murphy BA, Netterville J *et al*: **Increased epidermal growth factor receptor gene copy number is associated with poor prognosis in head and neck squamous cell carcinomas**. *J Clin Oncol* 2006, **24**(25):4170-4176.
 12. Temam S, Kawaguchi H, El-Naggar AK, Jelinek J, Tang H, Liu DD, Lang W, Issa JP, Lee JJ, Mao L: **Epidermal growth factor receptor copy number alterations correlate with poor clinical outcome in patients with head and neck squamous cancer**. *J Clin Oncol* 2007, **25**(16):2164-2170.
 13. Bonner JA, Harari PM, Giralt J, Cohen RB, Jones CU, Sur RK, Raben D, Baselga J, Spencer SA, Zhu J *et al*: **Radiotherapy plus cetuximab for locoregionally advanced head and neck cancer: 5-year survival data from a phase 3 randomised trial, and relation between cetuximab-induced rash and survival**. *Lancet Oncol* 2010, **11**(1):21-28.
 14. Hanahan D, Weinberg RA: **Hallmarks of cancer: the next generation**. *Cell* 2011, **144**(5):646-674.
 15. Hodi FS, O'Day SJ, McDermott DF, Weber RW, Sosman JA, Haanen JB, Gonzalez R, Robert C, Schadendorf D, Hassel JC *et al*: **Improved survival with ipilimumab in patients with metastatic melanoma**. *N Engl J Med* 2010, **363**(8):711-723.
 16. Schadendorf D, Hodi FS, Robert C, Weber JS, Margolin K, Hamid O, Patt D, Chen TT, Berman DM, Wolchok JD: **Pooled Analysis of Long-Term Survival Data From Phase II and Phase III Trials of Ipilimumab in Unresectable or Metastatic Melanoma**. *J Clin Oncol* 2015, **33**(17):1889-1894.
 17. Ferris RL, Blumenschein G, Jr., Fayette J, Guigay J, Colevas AD, Licitra L, Harrington K, Kasper S, Vokes EE, Even C *et al*: **Nivolumab for Recurrent Squamous-Cell Carcinoma of the Head and Neck**. *N Engl J Med* 2016, **375**(19):1856-1867.
 18. Cohen EEW, Soulieres D, Le Tourneau C, Dinis J, Licitra L, Ahn MJ, Soria A, Machiels JP, Mach N, Mehra R *et al*: **Pembrolizumab versus methotrexate, docetaxel, or cetuximab for recurrent or metastatic head-and-neck squamous cell carcinoma (KEYNOTE-040): a randomised, open-label, phase 3 study**. *Lancet* 2019, **393**(10167):156-167.
 19. Syn NL, Teng MWL, Mok TSK, Soo RA: **De-novo and acquired resistance to immune checkpoint targeting**. *Lancet Oncol* 2017, **18**(12):e731-e741.
 20. Binnewies M, Roberts EW, Kersten K, Chan V, Fearon DF, Merad M, Coussens

- LM, Gabilovich DI, Ostrand-Rosenberg S, Hedrick CC *et al*: **Understanding the tumor immune microenvironment (TIME) for effective therapy.** *Nat Med* 2018, **24**(5):541-550.
21. Tumei PC, Harview CL, Yearley JH, Shintaku IP, Taylor EJ, Robert L, Chmielowski B, Spasic M, Henry G, Ciobanu V *et al*: **PD-1 blockade induces responses by inhibiting adaptive immune resistance.** *Nature* 2014, **515**(7528):568-571.
22. Duan Q, Zhang H, Zheng J, Zhang L: **Turning Cold into Hot: Firing up the Tumor Microenvironment.** *Trends Cancer* 2020, **6**(7):605-618.
23. Nishikawa H, Sakaguchi S: **Regulatory T cells in tumor immunity.** *Int J Cancer* 2010, **127**(4):759-767.
24. Pan Y, Yu Y, Wang X, Zhang T: **Tumor-Associated Macrophages in Tumor Immunity.** *Front Immunol* 2020, **11**:583084.
25. Wculek SK, Cueto FJ, Mujal AM, Melero I, Krummel MF, Sancho D: **Dendritic cells in cancer immunology and immunotherapy.** *Nat Rev Immunol* 2020, **20**(1):7-24.
26. Newman AM, Liu CL, Green MR, Gentles AJ, Feng W, Xu Y, Hoang CD, Diehn M, Alizadeh AA: **Robust enumeration of cell subsets from tissue expression profiles.** *Nat Methods* 2015, **12**(5):453-457.
27. Gentles AJ, Newman AM, Liu CL, Bratman SV, Feng W, Kim D, Nair VS, Xu Y, Khuong A, Hoang CD *et al*: **The prognostic landscape of genes and infiltrating immune cells across human cancers.** *Nat Med* 2015, **21**(8):938-945.
28. Engblom C, Pfirschke C, Pittet MJ: **The role of myeloid cells in cancer therapies.** *Nat Rev Cancer* 2016, **16**(7):447-462.
29. Snyder A, Makarov V, Merghoub T, Yuan J, Zaretsky JM, Desrichard A, Walsh LA, Postow MA, Wong P, Ho TS *et al*: **Genetic basis for clinical response to CTLA-4 blockade in melanoma.** *N Engl J Med* 2014, **371**(23):2189-2199.
30. Le DT, Uram JN, Wang H, Bartlett BR, Kemberling H, Eyring AD, Skora AD, Lubner BS, Azad NS, Laheru D *et al*: **PD-1 Blockade in Tumors with Mismatch-Repair Deficiency.** *N Engl J Med* 2015, **372**(26):2509-2520.
31. Rizvi NA, Hellmann MD, Snyder A, Kvistborg P, Makarov V, Havel JJ, Lee W, Yuan J, Wong P, Ho TS *et al*: **Cancer immunology. Mutational landscape determines sensitivity to PD-1 blockade in non-small cell lung cancer.** *Science* 2015, **348**(6230):124-128.
32. Venkatesan S, Angelova M, Puttick C, Zhai H, Caswell DR, Lu WT, Dietzen M, Galanos P, Evangelou K, Bellelli R *et al*: **Induction of APOBEC3 Exacerbates DNA Replication Stress and Chromosomal Instability in Early Breast and**

- Lung Cancer Evolution.** *Cancer Discov* 2021, **11**(10):2456-2473.
33. Zaretsky JM, Garcia-Diaz A, Shin DS, Escuin-Ordinas H, Hugo W, Hu-Lieskovan S, Torrejon DY, Abril-Rodriguez G, Sandoval S, Barthly L *et al*: **Mutations Associated with Acquired Resistance to PD-1 Blockade in Melanoma.** *New England Journal of Medicine* 2016, **375**(9):819-829.
34. Gattinoni L, Ji Y, Restifo NP: **Wnt/beta-catenin signaling in T-cell immunity and cancer immunotherapy.** *Clin Cancer Res* 2010, **16**(19):4695-4701.
35. Garon EB, Rizvi NA, Hui R, Leighl N, Balmanoukian AS, Eder JP, Patnaik A, Aggarwal C, Gubens M, Horn L *et al*: **Pembrolizumab for the treatment of non-small-cell lung cancer.** *N Engl J Med* 2015, **372**(21):2018-2028.
36. Chow LQM, Haddad R, Gupta S, Mahipal A, Mehra R, Tahara M, Berger R, Eder JP, Burtness B, Lee SH *et al*: **Antitumor Activity of Pembrolizumab in Biomarker-Unselected Patients With Recurrent and/or Metastatic Head and Neck Squamous Cell Carcinoma: Results From the Phase Ib KEYNOTE-012 Expansion Cohort.** *J Clin Oncol* 2016, **34**(32):3838-3845.
37. Geiss GK, Bumgarner RE, Birditt B, Dahl T, Dowidar N, Dunaway DL, Fell HP, Ferree S, George RD, Grogan T *et al*: **Direct multiplexed measurement of gene expression with color-coded probe pairs.** *Nat Biotechnol* 2008, **26**(3):317-325.
38. Frampton GM, Fichtenholtz A, Otto GA, Wang K, Downing SR, He J, Schnall-Levin M, White J, Sanford EM, An P *et al*: **Development and validation of a clinical cancer genomic profiling test based on massively parallel DNA sequencing.** *Nat Biotechnol* 2013, **31**(11):1023-1031.
39. Krishnaswamy S, Spitzer MH, Mingueneau M, Bendall SC, Litvin O, Stone E, Pe'er D, Nolan GP: **Systems biology. Conditional density-based analysis of T cell signaling in single-cell data.** *Science* 2014, **346**(6213):1250689.
40. Subramanian A, Tamayo P, Mootha VK, Mukherjee S, Ebert BL, Gillette MA, Paulovich A, Pomeroy SL, Golub TR, Lander ES *et al*: **Gene set enrichment analysis: a knowledge-based approach for interpreting genome-wide expression profiles.** *Proc Natl Acad Sci U S A* 2005, **102**(43):15545-15550.
41. Burtness B, Harrington KJ, Greil R, Soulieres D, Tahara M, de Castro G, Jr., Psyrrri A, Baste N, Neupane P, Bratland A *et al*: **Pembrolizumab alone or with chemotherapy versus cetuximab with chemotherapy for recurrent or metastatic squamous cell carcinoma of the head and neck (KEYNOTE-048): a randomised, open-label, phase 3 study.** *Lancet* 2019, **394**(10212):1915-1928.
42. Kalbasi A, Ribas A: **Tumour-intrinsic resistance to immune checkpoint blockade.** *Nat Rev Immunol* 2020, **20**(1):25-39.

43. Chen DS, Mellman I: **Oncology meets immunology: the cancer-immunity cycle.** *Immunity* 2013, **39**(1):1-10.
44. Jansen CS, Prokhnevskaya N, Master VA, Sanda MG, Carlisle JW, Bilen MA, Cardenas M, Wilkinson S, Lake R, Sowalsky AG *et al*: **An intra-tumoral niche maintains and differentiates stem-like CD8 T cells.** *Nature* 2019, **576**(7787):465-470.
45. Basham TY, Merigan TC: **Recombinant interferon-gamma increases HLA-DR synthesis and expression.** *J Immunol* 1983, **130**(4):1492-1494.
46. Lee JH, Shklovskaya E, Lim SY, Carlino MS, Menzies AM, Stewart A, Pedersen B, Irvine M, Alavi S, Yang JYH *et al*: **Transcriptional downregulation of MHC class I and melanoma de- differentiation in resistance to PD-1 inhibition.** *Nat Commun* 2020, **11**(1):1897.
47. Concha-Benavente F, Srivastava RM, Trivedi S, Lei Y, Chandran U, Seethala RR, Freeman GJ, Ferris RL: **Identification of the Cell-Intrinsic and - Extrinsic Pathways Downstream of EGFR and IFN γ That Induce PD-L1 Expression in Head and Neck Cancer.** *Cancer Res* 2016, **76**(5):1031-1043.
48. Leibowitz MS, Srivastava RM, Andrade Filho PA, Egloff AM, Wang L, Seethala RR, Ferrone S, Ferris RL: **SHP2 is overexpressed and inhibits pSTAT1-mediated APM component expression, T-cell attracting chemokine secretion, and CTL recognition in head and neck cancer cells.** *Clin Cancer Res* 2013, **19**(4):798-808.
49. Galluzzi L, Buque A, Kepp O, Zitvogel L, Kroemer G: **Immunological Effects of Conventional Chemotherapy and Targeted Anticancer Agents.** *Cancer Cell* 2015, **28**(6):690-714.
50. Gandhi L, Rodriguez-Abreu D, Gadgeel S, Esteban E, Felip E, De Angelis F, Domine M, Clingan P, Hochmair MJ, Powell SF *et al*: **Pembrolizumab plus Chemotherapy in Metastatic Non-Small-Cell Lung Cancer.** *N Engl J Med* 2018, **378**(22):2078-2092.
51. Janjigian YY, Shitara K, Moehler M, Garrido M, Salman P, Shen L, Wyrwicz L, Yamaguchi K, Skoczylas T, Campos Bragagnoli A *et al*: **First-line nivolumab plus chemotherapy versus chemotherapy alone for advanced gastric, gastro-oesophageal junction, and oesophageal adenocarcinoma (CheckMate 649): a randomised, open-label, phase 3 trial.** *Lancet* 2021, **398**(10294):27-40.
52. Lizotte PH, Hong RL, Luster TA, Cavanaugh ME, Taus LJ, Wang S, Dhaneshwar A, Mayman N, Yang A, Kulkarni M *et al*: **A High-Throughput Immune-Oncology Screen Identifies EGFR Inhibitors as Potent Enhancers**

- of Antigen-Specific Cytotoxic T-lymphocyte Tumor Cell Killing. *Cancer Immunol Res* 2018, **6**(12):1511-1523.**
53. Guo Y, Ahn MJ, Chan A, Wang CH, Kang JH, Kim SB, Bello M, Arora RS, Zhang Q, He X *et al*: **Afatinib versus methotrexate as second-line treatment in Asian patients with recurrent or metastatic squamous cell carcinoma of the head and neck progressing on or after platinum-based therapy (LUX-Head & Neck 3): an open-label, randomised phase III trial.** *Ann Oncol* 2019, **30**(11):1831-1839.
54. Machiels J-PH, Haddad RI, Fayette J, Licitra LF, Tahara M, Vermorken JB, Clement PM, Gauler T, Cupissol D, Grau JJ *et al*: **Afatinib versus methotrexate as second-line treatment in patients with recurrent or metastatic squamous-cell carcinoma of the head and neck progressing on or after platinum-based therapy (LUX-Head & Neck 1): an open-label, randomised phase 3 trial.** *The Lancet Oncology* 2015, **16**(5):583-594.
55. Shannon P, Markiel A, Ozier O, Baliga NS, Wang JT, Ramage D, Amin N, Schwikowski B, Ideker T: **Cytoscape: a software environment for integrated models of biomolecular interaction networks.** *Genome Res* 2003, **13**(11):2498-2504.
56. Merico D, Isserlin R, Stueker O, Emili A, Bader GD: **Enrichment map: a network-based method for gene-set enrichment visualization and interpretation.** *PLoS One* 2010, **5**(11):e13984.
57. Doncheva NT, Morris JH, Gorodkin J, Jensen LJ: **Cytoscape StringApp: Network Analysis and Visualization of Proteomics Data.** *J Proteome Res* 2019, **18**(2):623-632.
58. Hoadley KA, Yau C, Hinoue T, Wolf DM, Lazar AJ, Drill E, Shen R, Taylor AM, Cherniack AD, Thorsson V *et al*: **Cell-of-Origin Patterns Dominate the Molecular Classification of 10,000 Tumors from 33 Types of Cancer.** *Cell* 2018, **173**(2):291-304 e296.
59. Emancipator K, Huang L, Aurora-Garg D, Bal T, Cohen EEW, Harrington K, Soulieres D, Le Tourneau C, Licitra L, Burtneess B *et al*: **Comparing programmed death ligand 1 scores for predicting pembrolizumab efficacy in head and neck cancer.** *Mod Pathol* 2021, **34**(3):532-541.
60. Litchfield K, Reading JL, Puttick C, Thakkar K, Abbosh C, Bentham R, Watkins TBK, Rosenthal R, Biswas D, Rowan A *et al*: **Meta-analysis of tumor- and T cell-intrinsic mechanisms of sensitization to checkpoint inhibition.** *Cell* 2021, **184**(3):596-614 e514.
61. House IG, Savas P, Lai J, Chen AXY, Oliver AJ, Teo ZL, Todd KL, Henderson MA, Giuffrida L, Petley EV *et al*: **Macrophage-Derived CXCL9 and**

- CXCL10 Are Required for Antitumor Immune Responses Following Immune Checkpoint Blockade.** *Clin Cancer Res* 2020, **26**(2):487-504.
62. Barry KC, Hsu J, Broz ML, Cueto FJ, Binnewies M, Combes AJ, Nelson AE, Loo K, Kumar R, Rosenblum MD *et al*: **A natural killer-dendritic cell axis defines checkpoint therapy-responsive tumor microenvironments.** *Nat Med* 2018, **24**(8):1178-1191.
63. Lee JJ, Kao KC, Chiu YL, Jung CJ, Liu CJ, Cheng SJ, Chang YL, Ko JY, Chia JS: **Enrichment of Human CCR6(+) Regulatory T Cells with Superior Suppressive Activity in Oral Cancer.** *J Immunol* 2017, **199**(2):467-476.
64. Barkal AA, Brewer RE, Markovic M, Kowarsky M, Barkal SA, Zaro BW, Krishnan V, Hatakeyama J, Dorigo O, Barkal LJ *et al*: **CD24 signalling through macrophage Siglec-10 is a target for cancer immunotherapy.** *Nature* 2019, **572**(7769):392-396.
65. Mowen KA, Tang J, Zhu W, Schurter BT, Shuai K, Herschman HR, David M: **Arginine methylation of STAT1 modulates IFNalpha/beta-induced transcription.** *Cell* 2001, **104**(5):731-741.
66. Gao J, Shi LZ, Zhao H, Chen J, Xiong L, He Q, Chen T, Roszik J, Bernatchez C, Woodman SE *et al*: **Loss of IFN-gamma Pathway Genes in Tumor Cells as a Mechanism of Resistance to Anti-CTLA-4 Therapy.** *Cell* 2016, **167**(2):397-404 e399.
67. Sacco AG, Chen R, Worden FP, Wong DJL, Adkins D, Swiecicki P, Chai-Ho W, Oppelt P, Ghosh D, Bykowski J *et al*: **Pembrolizumab plus cetuximab in patients with recurrent or metastatic head and neck squamous cell carcinoma: an open-label, multi-arm, non-randomised, multicentre, phase 2 trial.** *Lancet Oncol* 2021, **22**(6):883-892.
68. Taylor MH, Lee CH, Makker V, Rasco D, Dutcus CE, Wu J, Stepan DE, Shumaker RC, Motzer RJ: **Phase IB/II Trial of Lenvatinib Plus Pembrolizumab in Patients With Advanced Renal Cell Carcinoma, Endometrial Cancer, and Other Selected Advanced Solid Tumors.** *J Clin Oncol* 2020, **38**(11):1154-1163.
69. Larkin J, Chiarion-Sileni V, Gonzalez R, Grob JJ, Rutkowski P, Lao CD, Cowey CL, Schadendorf D, Wagstaff J, Dummer R *et al*: **Five-Year Survival with Combined Nivolumab and Ipilimumab in Advanced Melanoma.** *N Engl J Med* 2019, **381**(16):1535-1546.
70. Motzer RJ, Tannir NM, McDermott DF, Aren Frontera O, Melichar B, Choueiri TK, Plimack ER, Barthelemy P, Porta C, George S *et al*: **Nivolumab plus Ipilimumab versus Sunitinib in Advanced Renal-Cell Carcinoma.** *N Engl J Med* 2018, **378**(14):1277-1290.

71. Hellmann MD, Paz-Ares L, Bernabe Caro R, Zurawski B, Kim SW, Carcereny Costa E, Park K, Alexandru A, Lupinacci L, de la Mora Jimenez E *et al*: **Nivolumab plus Ipilimumab in Advanced Non-Small-Cell Lung Cancer.** *N Engl J Med* 2019, **381**(21):2020-2031.
72. Ferris RL, Haddad R, Even C, Tahara M, Dvorkin M, Ciuleanu TE, Clement PM, Mesia R, Kutukova S, Zholudeva L *et al*: **Durvalumab with or without tremelimumab in patients with recurrent or metastatic head and neck squamous cell carcinoma: EAGLE, a randomized, open-label phase III study.** *Ann Oncol* 2020, **31**(7):942-950.
73. Argiris A, Harrington K, Tahara M, Ferris RL, Gillison M, Fayette J, Daste A, Koralewski P, Mesia Nin R, Saba NF *et al*: **LBA36 Nivolumab (N) + ipilimumab (I) vs EXTREME as first-line (1L) treatment (tx) for recurrent/metastatic squamous cell carcinoma of the head and neck (R/M SCCHN): Final results of CheckMate 651.** *Ann Oncol* 2021, **32**:S1310-S1311.
74. Harrington KJ, Kong A, Mach N, Chesney JA, Fernandez BC, Rischin D, Cohen EEW, Radcliffe HS, Gumuscu B, Cheng J *et al*: **Talimogene Laherparepvec and Pembrolizumab in Recurrent or Metastatic Squamous Cell Carcinoma of the Head and Neck (MASTERKEY-232): A Multicenter, Phase 1b Study.** *Clin Cancer Res* 2020, **26**(19):5153-5161.
75. Massarelli E, William W, Johnson F, Kies M, Ferrarotto R, Guo M, Feng L, Lee JJ, Tran H, Kim YU *et al*: **Combining Immune Checkpoint Blockade and Tumor-Specific Vaccine for Patients With Incurable Human Papillomavirus 16-Related Cancer: A Phase 2 Clinical Trial.** *JAMA Oncol* 2019, **5**(1):67-73.
76. Rodriguez CP, Wu QV, Voutsinas J, Fromm JR, Jiang X, Pillarisetty VG, Lee SM, Santana-Davila R, Goulart B, Baik CS *et al*: **A Phase II Trial of Pembrolizumab and Vorinostat in Recurrent Metastatic Head and Neck Squamous Cell Carcinomas and Salivary Gland Cancer.** *Clin Cancer Res* 2020, **26**(4):837-845.
77. Uppaluri R, Campbell KM, Egloff AM, Zolkind P, Skidmore ZL, Nussenbaum B, Paniello RC, Rich JT, Jackson R, Pipkorn P *et al*: **Neoadjuvant and Adjuvant Pembrolizumab in Resectable Locally Advanced, Human Papillomavirus-Unrelated Head and Neck Cancer: A Multicenter, Phase II Trial.** *Clin Cancer Res* 2020, **26**(19):5140-5152.
78. Cristescu R, Mogg R, Ayers M, Albright A, Murphy E, Yearley J, Sher X, Liu XQ, Lu H, Nebozhyn M *et al*: **Pan-tumor genomic biomarkers for PD-1 checkpoint blockade-based immunotherapy.** *Science* 2018, **362**(6411).
79. Tu HF, Ko CJ, Lee CT, Lee CF, Lan SW, Lin HH, Lin HY, Ku CC, Lee DY,

- Chen IC *et al*: **Afatinib Exerts Immunomodulatory Effects by Targeting the Pyrimidine Biosynthesis Enzyme CAD**. *Cancer Res* 2021, **81**(12):3270-3282.
80. Yang JC, Gadgeel SM, Sequist LV, Wu CL, Papadimitrakopoulou VA, Su WC, Fiore J, Saraf S, Raftopoulos H, Patnaik A: **Pembrolizumab in Combination With Erlotinib or Gefitinib as First-Line Therapy for Advanced NSCLC With Sensitizing EGFR Mutation**. *J Thorac Oncol* 2019, **14**(3):553-559.
81. Yang JC, Shepherd FA, Kim DW, Lee GW, Lee JS, Chang GC, Lee SS, Wei YF, Lee YG, Laus G *et al*: **Osimertinib Plus Durvalumab versus Osimertinib Monotherapy in EGFR T790M-Positive NSCLC following Previous EGFR TKI Therapy: CAURAL Brief Report**. *J Thorac Oncol* 2019, **14**(5):933-939.
82. Khoja L, Day D, Wei-Wu Chen T, Siu LL, Hansen AR: **Tumour- and class-specific patterns of immune-related adverse events of immune checkpoint inhibitors: a systematic review**. *Ann Oncol* 2017, **28**(10):2377-2385.
83. Gohil SH, Iorgulescu JB, Braun DA, Keskin DB, Livak KJ: **Applying high-dimensional single-cell technologies to the analysis of cancer immunotherapy**. *Nat Rev Clin Oncol* 2021, **18**(4):244-256.
84. Lundberg E, Borner GHH: **Spatial proteomics: a powerful discovery tool for cell biology**. *Nat Rev Mol Cell Biol* 2019, **20**(5):285-302.
85. Ignatiadis M, Sledge GW, Jeffrey SS: **Liquid biopsy enters the clinic - implementation issues and future challenges**. *Nat Rev Clin Oncol* 2021, **18**(5):297-312.
86. The Cancer Genome Atlas N, Lawrence MS, Sougnez C, Lichtenstein L, Cibulskis K, Lander E, Gabriel SB, Getz G, Ally A, Balasundaram M *et al*: **Comprehensive genomic characterization of head and neck squamous cell carcinomas**. *Nature* 2015, **517**:576.
87. Deng J, Wang ES, Jenkins RW, Li S, Dries R, Yates K, Chhabra S, Huang W, Liu H, Aref AR *et al*: **CDK4/6 Inhibition Augments Antitumor Immunity by Enhancing T-cell Activation**. *Cancer Discov* 2018, **8**(2):216-233.
88. Schaer DA, Beckmann RP, Dempsey JA, Huber L, Forest A, Amaladas N, Li Y, Wang YC, Rasmussen ER, Chin D *et al*: **The CDK4/6 Inhibitor Abemaciclib Induces a T Cell Inflamed Tumor Microenvironment and Enhances the Efficacy of PD-L1 Checkpoint Blockade**. *Cell reports* 2018, **22**(11):2978-2994.
89. Jerby-Arnon L, Shah P, Cuoco MS, Rodman C, Su MJ, Melms JC, Leeson R, Kanodia A, Mei S, Lin JR *et al*: **A Cancer Cell Program Promotes T Cell Exclusion and Resistance to Checkpoint Blockade**. *Cell* 2018, **175**(4):984-997 e924.

Chapter 10 Appendix



10.1 Journal papers related with this dissertation

1. Hsiang-Fong Kao, Bin-Chi Liao, Yen-Lin Huang, Huai-Cheng Huang, Chun-Nan Chen, Tseng-Cheng Chen, Yuan-Jing Hong, Ching-Yi Chang, Jean-San Chia, Ruey-Long Hong, **Afatinib and Pembrolizumab for Recurrent or Metastatic Head and Neck Squamous Cell Carcinoma (ALPHA Study): A Phase II Study with Biomarker Analysis.** *Clinical Cancer Research* 2022, 28(8):1560-1571

10.2 Open data of the study

The mRNA analysis data by Nanostring platform could be obtained in Gene Expression Omnibus (<https://www.ncbi.nlm.nih.gov/geo/>; GEO Accession No. GSE190575).